1976

Many-Body Perturbation Theory Applied to Molecules: Analysis and Correlation Energy Calculation for Li_2, N_2, and H_3

David L. Freeman
University of Rhode Island, dfreeman@uri.edu

Martin Karplus

Citation/Publisher Attribution

Freeman, D. L., & Karplus, M. (1976). Many-body Perturbation Theory Applied to Molecules: Analysis and Correlation Energy Calculation for Li2, N2, and H3. *J. Chem. Phys.*, *64*(6), 2641- 2659. doi: 10.1063/1.432518
Available at: http://dx.doi.org/10.1063/1.432518

Many-Body Perturbation Theory Applied to Molecules: Analysis and Correlation Energy Calculation for Li_2, N_2, and H_3

Manybody perturbation theory applied to molecules: Analysis and correlation energy calculation for Li2, N2, and H3

David L. Freemen and Martin Karplus

Citation: J. Chem. Phys. **64**, 2641 (1976); doi: 10.1063/1.432518
View online: http://dx.doi.org/10.1063/1.432518
View Table of Contents: http://jcp.aip.org/resource/1/JCPSA6/v64/i6
Published by the American Institute of Physics.

Many-body perturbation theory applied to molecules: Analysis and correlation energy calculation for Li_2, N_2, and H_3*

David L. Freemen† and Martin Karplus

Department of Chemistry, Harvard University, Cambridge, Massachusetts 02138
(Received 11 July 1975)

The correlation problem is analyzed in terms of Goldstone diagrammatic perturbation theory. A hole-line expansion for the correlation energy is defined and used with matrix partitioning techniques to determine the diagrams contributing to various forms of pair theory and to configuration interaction treatments of the usual type. The presence of certain terms in the double excitation configuration interaction formulation that cancel in higher order is demonstrated. The nature of various approximations to the correlation correction is determined. To illustrate the analysis, certain of the approximations are used in correlation energy calculations with multicenter Slater basis sets on Li_2, N_2, and H_3. Comparison with complete configuration interaction calculations are made for Li_2 and H_3; the diagrammatic calculation, which is much simpler than a full CI treatment, is found to be a good approximation to the latter.

I. INTRODUCTION

The most commonly used method for *ab initio* calculations on the properties of many-electron atomic and molecular systems is based on the Hartree–Fock equations.[1] The popularity of the Hartree–Fock method is due to the possibility of solving the equations for a large variety of systems, and the success achieved in calculating various of their properties, including moments of the charge distributions and total energies. Unfortunately the Hartree–Fock method is not sufficiently accurate for other important properties, such as molecular binding energies and atomic or molecular electron affinities. Techniques for introducing electron correlation effects are therefore needed. Recently, a number of ways have been developed and implemented for determining the correlation correction in atoms and simple molecules. Among the approximations that have been used are the configuration interaction method,[2] the atomic Bethe–Goldstone equations,[3] the many-electron theory of Sinanoğlu,[4] Goldstone diagrammatic perturbation theory,[5] coupled pair many-electron theory,[6] and the many-body Green's function approach.[7,8] Of the various techniques, the configuration interaction method is conceptually the most simple and the most widely employed. However, the success achieved by some of the many-body methods in the rapid and accurate calculation of atomic correlation effects makes desirable their extension to molecular problems.

Most of the available molecular calculations have been performed for systems that can be treated with a one-center expansion. These include the studies of H_2 by Kelly,[9,10] the work on diatomic hydrides by Das and coworkers,[11,12] and a number of investigations of polyatomic hydrides.[13–15] Although these calculations have given useful results, the more general application of many-body methods to molecules necessitates a search for other than one-center basis sets. Some progress has been made in this area. Dutta, Dutta, and Das[16] used H_2^+ solutions as basis functions for H_2 and more recently, diatomic hydrides have been studied with multicenter Slater basis sets.[17–21]

In addition to the need for more flexible basis functions, the greater complexity of the molecular problem requires that simplifications be introduced into the many-body treatment. To obtain a better understanding of the important diagrammatic contributions to the correlation correction in molecules, we present in this paper an analysis of Goldstone many-body perturbation theory and apply it with extended Slater-type-orbital basis sets to Li_2, N_2, and H_3.

The connections between the various many-body methods have been discussed by Freed[22–24] and by Kelly *et al.*[25,26] In what follows we examine the relationships by a somewhat different approach. We start with Nesbet's variation-perturbation formulation,[3] which utilizes a configurational expansion. By means of matrix partitioning techniques,[27] we analyze the relation between Nesbet's treatment and Goldstone diagrammatic perturbation theory.[28] We are able then to determine the connection with the more usual CI expansion and some of the other many-body methods.

To establish notation, we state the correlation problem in terms of Goldstone diagrams in Sec. II. In Sec. III we introduce an expansion for the correlation energy in terms of the hole lines of the Goldstone diagrams. We use this hole-line expansion to develop the connection between Goldstone perturbation theory and the "Bethe–Goldstone equations" of Nesbet. We then show which diagrams are included in the CI expansion. The discussion given in Sec. III is limited to the ground states of closed-shell systems. In Sec. IV we briefly consider the extension to open-shell systems, and test the many-body approximations to the correlation energy by calculation on Li_2, N_2, and H_3.

II. THE DIAGRAMMATIC FORMULATION OF THE CORRELATION CORRECTION

To introduce the necessary notation, we outline the many-body perturbation theory for the correlation correction to the energy and wavefunction. We partition the full Hamiltonian, H, for an N-electron atomic or

molecular system as

$$H = H_0 + H' . \tag{1}$$

In Eq. (1), H_0 is the Hartree–Fock Hamiltonian defined by

$$H_0 = \sum_{i=1}^{N} h(i) = \sum_{i=1}^{N} [t(i) + v_{HF}(i)] , \tag{2}$$

where

$$t(i)\varphi_k(i) = \left[-\frac{\nabla_i^2}{2} - \sum_\alpha \frac{Z_\alpha}{|\mathbf{R}_\alpha - \mathbf{r}_i|} \right] \varphi_k(i) = \epsilon_k \varphi_k(i) \tag{3}$$

and

$$v_{HF}(i)\varphi_k(i) = \sum_{\beta=1}^{N} [\langle \varphi_\beta(j) | v(i,j) | \varphi_\beta(j) \rangle \varphi_k(i) - \langle \varphi_\beta(j) | v(i,j) | \varphi_k(j) \rangle \varphi_\beta(i)] , \tag{4}$$

where $\{\phi_i\}$, and $\{\epsilon_i\}$ are the eigenfunctions and eigenvalues of the Hartree–Fock Hamiltonian $h(i)$, Z_α is the charge on nucleus α located at $\mathbf{R}_\alpha$, i and $\mathbf{r}_i$ represent the coordinates of electron i, $v(i,j)$ is the electron–electron interaction, and $v_{HF}(i)$ is the one-particle Hartree–Fock potential. From Eqs. (1) and (2), H' is given by

$$H' = \frac{1}{2} \sum_{i,j} v(i,j) - V_{HF} , \tag{5}$$

where

$$V_{HF} = \sum_{i=1}^{N} v_{HF}(i) . \tag{6}$$

We define $|\Phi_0\rangle$ as the Hartree–Fock ground state and let $|\Psi\rangle$ be the exact ground-state, which is an eigenfunction of the full Hamiltonian. The function $|\Phi_0\rangle$ is a single Slater determinant constructed from the N lowest occupied Hartree–Fock spin orbitals. We write $|\Psi\rangle$ in the form

$$|\Psi\rangle = |\Phi_0\rangle + |\chi\rangle \tag{7}$$

and use intermediate normalization

$$\langle \Phi_0 | \Phi_0 \rangle = 1 , \quad \langle \Phi_0 | \Psi \rangle = 1 \tag{8}$$

with

$$\langle \Phi_0 | \chi \rangle = 0 . \tag{9}$$

If E is the exact ground-state eigenvalue of the full Hamiltonian, H, and E_0 is the Hartree–Fock energy, defined by

$$E_0 = \langle \Phi_0 | H | \Phi_0 \rangle , \tag{10}$$

we have

$$E = \langle \Phi_0 | H | \psi \rangle = E_0 + \Delta E , \tag{11}$$

where

$$\Delta E = \langle \Phi_0 | H' | \chi \rangle \tag{12}$$

The energy shift, ΔE, is called the correlation energy and $|\chi\rangle$ the correlation part of the wavefunction.

To solve the correlation problem perturbatively, we take the Hartree–Fock Hamiltonian, H_0, as the zeroth-order Hamiltonian and treat H' as a perturbation. If we sum the Rayleigh–Schrödinger perturbation series to a given order, we obtain the correlation energy or the correlation part of the wavefunction to that order. For example, the energy through second order is

$$E^2 = E_0 + \Delta E^2 = E_0^0 + \langle \Phi_0 | H' | \Phi_0 \rangle + \sum_{\alpha\beta rs} \frac{|\langle \Phi_{\alpha\beta}^{rs} | H' | \Phi_0 \rangle|^2}{E_0^0 - E_{\alpha\beta,rs}^0} , \tag{13}$$

where

$$E_0^0 = \langle \Phi_0 | H_0 | \Phi_0 \rangle = \sum_{\alpha=1}^{N} \epsilon_\alpha \tag{14}$$

$$E_{\alpha\beta,rs}^0 = \langle \Phi_{\alpha\beta}^{rs} | H_0 | \Phi_{\alpha\beta}^{rs} \rangle = E_0 + (\epsilon_r + \epsilon_s - \epsilon_\alpha - \epsilon_\beta) \tag{15}$$

and $|\Phi_{\alpha\beta}^{rs}\rangle$ represents a determinant with occupied spin orbitals α, β excited into virtual spin orbitals r, s. We use Greek letters α, β, γ, δ to represent spin orbitals occupied in the Hartree–Fock ground state (hole states) and latin letters r, s, t, u to represent the virtual spin orbitals (particle states); the letters i, j, k, l represent either occupied or virtual orbitals. The wavefunction through first order is given by

$$|\Psi\rangle = |\Phi_0\rangle + |\Phi_1\rangle = |\Phi_0\rangle + \sum_{\alpha\beta rs} \frac{\langle \Phi_0 | H' | \Phi_{\alpha\beta}^{rs} \rangle | \Phi_{\alpha\beta}^{rs} \rangle}{E_0^0 - E_{\alpha\beta,rs}^0} . \tag{16}$$

Evaluating the matrix elements of Eq. (13) and (16), we obtain

$$E^2 = E_0 + \Delta E^2 = \sum_{\alpha=1}^{N} \epsilon_\alpha - \sum_{\alpha\beta} \langle \alpha\beta | v | \tilde{\alpha\beta} \rangle + \sum_{\alpha\beta rs} \frac{\langle rs | v | \tilde{\alpha\beta} \rangle \langle \alpha\beta | v | rs \rangle}{(\epsilon_\alpha + \epsilon_\beta - \epsilon_r - \epsilon_s)} \tag{17}$$

and

$$|\Phi_1\rangle = \sum_{\alpha\beta rs} \frac{\langle rs | v | \tilde{\alpha\beta} \rangle}{(\epsilon_\alpha + \epsilon_\beta - \epsilon_r - \epsilon_s)} |\Phi_{\alpha\beta}^{rs}\rangle , \tag{18}$$

where

$$\langle rs | v | \tilde{\alpha\beta} \rangle = \langle rs | v | \alpha\beta \rangle - \langle rs | v | \beta\alpha \rangle . \tag{19}$$

In Eqs. (17) and (18) we sum over distinct terms only. (This eliminates a factor of $\frac{1}{2}$ that appears in the corresponding equations with the sums going over all values in the indices.) For example, Eq. (17) includes only one of the terms

$$\frac{\langle rs | v | \tilde{\alpha\beta} \rangle \langle \alpha\beta | v | rs \rangle}{(\epsilon_\alpha + \epsilon_\beta - \epsilon_r - \epsilon_s)}$$

and

$$\frac{\langle sr | v | \tilde{\beta\alpha} \rangle \langle \beta\alpha | v | sr \rangle}{(\epsilon_\alpha + \epsilon_\beta - \epsilon_r - \epsilon_s)}$$

but not both. Throughout this paper we assume that any sum performed over spin-orbital labels is restricted to sums over distinct configurations.

We see from the definition of the correlation energy [Eqs. (11)–(13)] that the first-order correction ($\langle \Phi_0 | H' | \Phi_0 \rangle$) is included in the Hartree–Fock energy, and the correlation energy, ΔE, has as its lowest order term the second-order correction.

In second-quantized form the Hamiltonian corresponding to Eq. (1) is

$$H_0 = \sum_i \epsilon_i c_i^\dagger c_i \tag{20}$$

$$H' = \sum_{i,j,k,l} \langle ij|v|kl\rangle c_i^\dagger c_j^\dagger c_l c_k - \sum_{i,j} \langle i|v_{\rm HF}|j\rangle c_i^\dagger c_j \,, \qquad (21)$$

where c_i, $c_i^\dagger$ are spin-orbital annihilation and creation operators, respectively, and the indices i, j, k, l go over both occupied and unoccupied spin orbitals. Following the standard rules given by Goldstone[28] and in various textbooks,[29] the perturbation operator H' given in Eq. (21) can be used to set up the linked cluster expansion for the correlation energy, ΔE, and the correlation part of the wavefunction, $|\chi\rangle$. Figures 1 and 2 show all the diagrams contributing to ΔE through third order for the present case in which the unperturbed function, $|\Phi_0\rangle$, is the single-determinant Hartree–Fock solution for the system.

III. THE CONNECTION BETWEEN THE CI EXPANSION AND THE GOLDSTONE DIAGRAMS

In this section, we first introduce a cluster expansion for the correlation energy and then analyze the various contributions.

A. A cluster (hole-line) expansion for the correlation energy

Although it is possible to determine the contributions to the Rayleigh–Schrödinger perturbation series in an order-by-order fashion, as illustrated in Figs. 1 and 2, one can make better use of diagrammatic theory by employing alternative expansions which may be more rapidly convergent. We introduce a cluster expansion for the energy whose first correction term is the so-called "pair theory" contribution. The cluster expansion we define is different from the Ursell expansion used by Čižek,[6] but is equivalent to Nesbet's "Hierarchy of Bethe-Goldstone Equations."[3] Unlike Nesbet, we express this expansion in terms of Goldstone diagrams. The use of diagrams enables us to see directly the connection between Nesbet's formulation of the correlation problem and the perturbation terms summed by Kelly.[5] The pair terms we consider are equivalent to the "exact pairs" of Sinanoğlu,[30,31] and to the decoupled contributions to the coupled pair theory of Čižek, Paldus, and Shavitt.[6,32] However, the higher order terms of each of these approaches are different, and it is an advantage of the diagrammatic formulation of the correlation problem that we can express them in a common language.

The cluster expansion is defined by

$$\Delta E = \sum_{h=1}^{N} E_h \,, \qquad (22)$$

where the h-body contribution to the correlation energy, E_h, is the sum of all diagrams with h independent hole lines. A diagram is said to have h independent hole lines if it has h and only h distinct hole labels on its hole lines. For example, in Fig. 3 the labeled diagrams (a), (b), and (c) have two independent hole lines, diagrams (d) and (e) have three independent hole lines, and diagram (f) has four independent hole lines. We note that the number of independent hole lines has nothing to do with the order of the diagram in perturbation theory; e.g., in Fig. 3 diagrams (b) and (f) are both third-order diagrams, but diagram (b) has two independent hole lines and diagram (f) has four independent hole lines. Equation (22) consists of a finite number of terms, since for any given system there are no diagrams with more independent hole lines than the number of electrons in the system. However, each E_h contribution represents a sum of an infinite set of diagrams. To avoid later confusion we define orders in

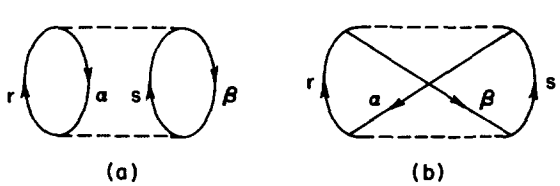

FIG. 1. The second-order energy diagrams.

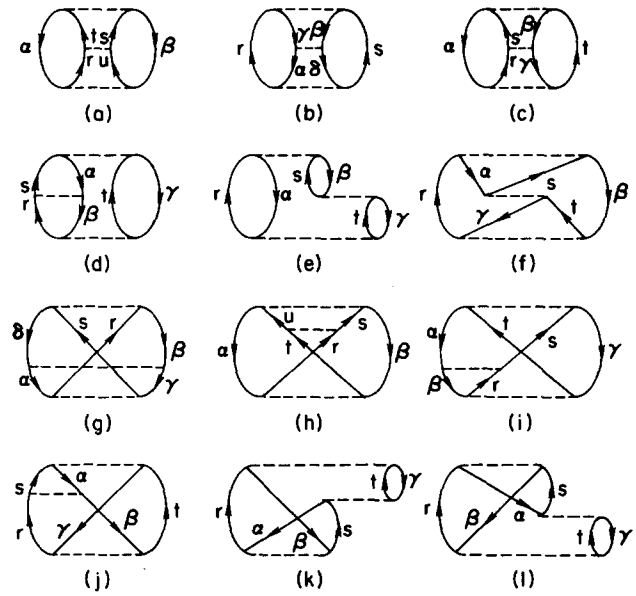

FIG. 2. The third-order energy diagrams.

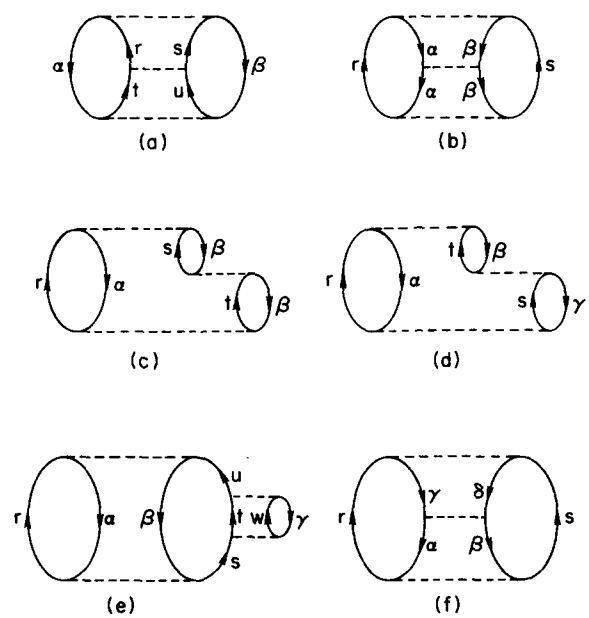

FIG. 3. Examples of diagrams contributing to the hole-line expansion [Eq. (22), see text].

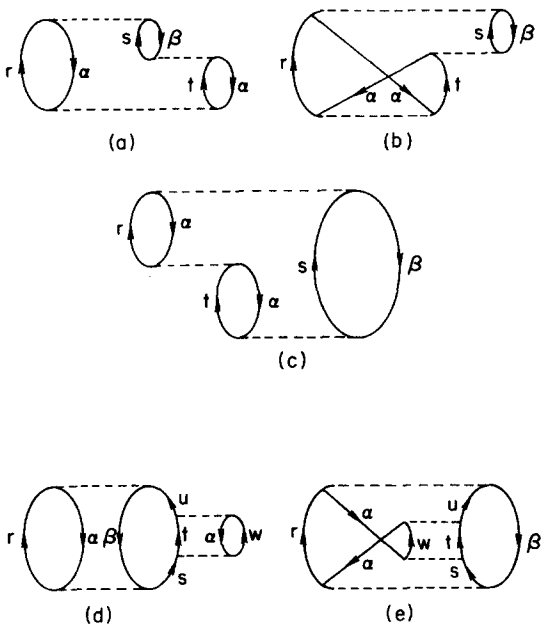

FIG. 4. Cancellation of hole-line diagrams (see text).

perturbation theory as "pert-orders" and orders in Eq. (22) as "hole-orders" or "h-orders."

Before examining the terms in Eq. (22) in detail, we introduce an important point that simplifies the diagrammatic analysis. Many of the diagrams cancel among themselves and we need compute only a small subclass of the total number of Goldstone diagrams. For example, the pair diagram in Fig. 4(a) and its exchange in Fig. 4(b) sum to zero; they differ only in sign, all of the matrix elements and energy denominators being the same, because the exchange involves lines with the same hole label, α. By contrast there is no exchange diagram that cancels with that given in Fig. 4(c). We must include the contribution from the diagram in Fig. 4(c), but it would simplify matters considerably if we could avoid the computation of diagrams such as Figs. 4(a) and 4(b) which sum to zero. Another example is given by the diagrams of Figs. 4(d) and its exchange in Fig. 4(e) which add to zero, for the same reasons as 4(a) and 4(b). Thus, we need a scheme whereby we can tell which diagrams to sum and which not to sum. One possibility would be to inspect all the diagrams and formally sum them to determine the cancellations. Such a procedure, which requires a complicated but illuminating analysis, has been described for the two-electron problem.[33] In this study which is concerned primarily with a comparison between diagrammatic and other many-body formulations, we shall take an indirect approach that is considerably simpler to apply. In each h-order approximation we derive the correlation contribution by the use of the configuration interaction formulation, and then show which diagrams sum to give the same result. Since different formulation for the correlation energy in a given approximation must be equal, all diagrams that do not appear in the final formula can be assumed to add to zero. We shall find, for example, when solving for the correlation energy in the pair approximation that the diagrams of Figs. 4(a), (b), (d), and (e) do not occur. We can therefore assume that they sum to zero without examining them individually.

B. The pair approximation, E_2

The second h-order term, E_2,

$$E_2 = \sum_{\alpha,\beta} \Delta E_{(\alpha\beta)} \tag{23}$$

is the sum over all pairs of hole states, (α, β) where $\Delta E_{(\alpha\beta)}$ is the pair energy for the pair (α, β). For a two-electron system, the total correlation energy relative to the Hartree–Fock energy is equal to

$$\Delta E = E_2 = \Delta E_{(\alpha\beta)} \tag{24}$$

since Brillouin's Theorem implies there are no E_1 contributions, and there are no higher h-order terms.

The solution to the pair problem is equivalent to solving for the energy of each pair of electrons in the presence of the other electrons in the system. For each pair of electrons, (α, β), in the many-electron system we write the configuration interaction wavefunction, $|\Psi_{\alpha\beta}\rangle$, as[3]

$$|\Psi_{\alpha\beta}\rangle = |\Phi_0\rangle + \sum_{rs} C_{\alpha\beta}^{rs} |\Phi_{\alpha\beta}^{rs}\rangle . \tag{25}$$

In Eq. (25) we have neglected single excitations; they are included later. It is convenient for the analysis to introduce the matrix equation corresponding to the Schrödinger equation

$$\mathbf{H}\mathbf{f} = E_{\alpha\beta}\mathbf{f} , \tag{26}$$

where $\mathbf{H}$ is the Hamiltonian matrix, $\mathbf{f}$ is the vector of the CI coefficients, and

$$E_{\alpha\beta} = E_0 + \Delta E_{(\alpha\beta)} . \tag{27}$$

We now partition $\mathbf{f}$ and $\mathbf{H}$ according to the equations

$$\mathbf{f} = (1, \mathbf{f}_2) = (1, \{C_{\alpha\beta}^{rs}\}) . \tag{28}$$

and

$$\mathbf{H} = \begin{bmatrix} E_0 & \mathbf{B} \\ \mathbf{B}^+ & \mathbf{D}' \end{bmatrix} , \tag{29}$$

where B is the row vector of matrix elements between the ground state and double excited states, $\mathbf{B}^+$ is its adjoint, and $\mathbf{D}'$ is the matrix of Hamiltonian matrix elements between the double excited states. Subtracting $E_0(\mathbf{I}\mathbf{f})$, where $\mathbf{I}$ is the unit matrix, from both sides of Eq. (26) we have

$$\begin{bmatrix} 0 & B \\ \mathbf{B}^+ & \mathbf{D} \end{bmatrix} \begin{bmatrix} 1 \\ \mathbf{f}_2 \end{bmatrix} = \Delta E_{(\alpha\beta)} \begin{bmatrix} 1 \\ \mathbf{f}_2 \end{bmatrix} , \tag{30}$$

where

$$\mathbf{D} = \mathbf{D}' - E_0\mathbf{I} . \tag{31}$$

Solving Eq. (30) for $\mathbf{f}_2$ and $\Delta E_{(\alpha\beta)}$ we obtain

$$f_2 = [\Delta E_{(\alpha\beta)}\mathbf{I} - \mathbf{D}]^{-1}\mathbf{B}^+ \tag{32}$$

and

$$\Delta E_{(\alpha\beta)} = \mathbf{B}[\Delta E_{(\alpha\beta)}\mathbf{I} - \mathbf{D}]^{-1}\mathbf{B}^+ . \tag{33}$$

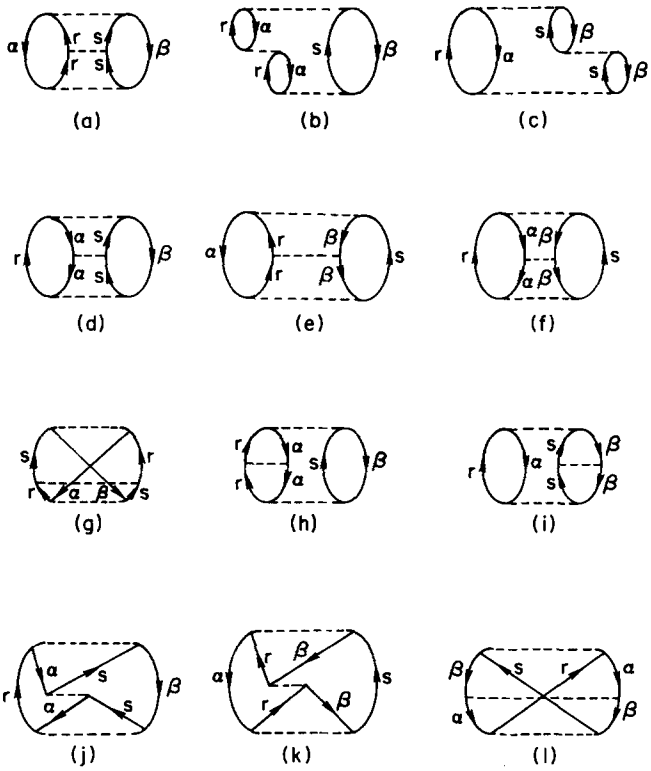

FIG. 5. The direct third pert-order diagrams that contribute to Epstein–Nesbet perturbation theory in second pert-order. Diagrams (a)–(f) are the Coulomb terms and (g)–(l) are the exchange contributions.

Equation (33) is in a convenient form for comparison with perturbation theory. To obtain the lowest-order result, we make the approximations

$$\Delta E_{(\alpha\beta)} \cong 0\,, \quad \mathbf{D} \cong \mathbf{d} \tag{34}$$

where $\mathbf{d}$ is the diagonal part of $\mathbf{D}$ with elements

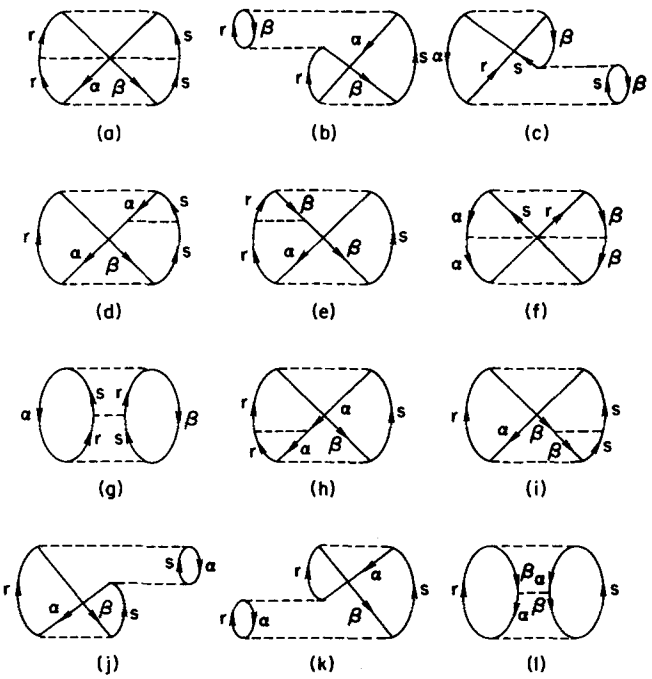

FIG. 6. The third pert-order exchange diagrams that contribute to second pert-order Epstein–Nesbet perturbation theory.

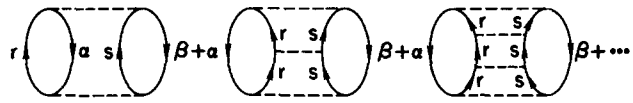

FIG. 7. The particle–particle ladder geometric series.

$$d_{rs}^{tu} = [\langle \Phi_{\alpha\beta}^{rs} | H | \Phi_{\alpha\beta}^{tu} \rangle - E_0]\delta_{rt}\delta_{su} \tag{35}$$

and we write Eq. (33) in the form

$$\Delta E_{(\alpha\beta)} \cong \Delta E_{(\alpha\beta)}^{d} = \mathrm{B}(1/-\mathbf{d})\mathrm{B}^{\dagger}. \tag{36}$$

Writing out the summations of Eq. (36) we have

$$\Delta E_{(\alpha\beta)}^{d} = \sum_{r,s} \frac{|\langle \Phi_{\alpha\beta}^{rs} | H' | \Phi_0 \rangle|^2}{E_0 - \langle \Phi_{\alpha\beta}^{rs} | H | \Phi_{\alpha\beta}^{rs} \rangle}\,. \tag{37}$$

As Claverie, Diner, and Malrieu[34] have pointed out very clearly, Eq. (37) can be obtained as the second pert-order energy for the (α, β) pair by choosing a partitioning of the Hamiltonian different from Eq. (20) and Eq. (21) and applying Rayleigh–Schrödinger perturbation theory to it. This form of perturbation theory is often referred to as "Epstein–Nesbet perturbation theory," and has been shown to converge more rapidly in certain applications. An alternative procedure for obtaining Eq. (37) is to begin with the second pert-order result given in Eq. (17) applied to a single pair (second hole-order) and sum certain classes of Goldstone diagrams to infinite pert-order. To do this we use the geometric summation technique first applied to atoms by Kelly.[5] We start with the second pert-order Coulomb and exchange diagrams in Figs. 1 and add to them interaction lines in such a way that the labels on a hole or particle line intersected by the added interaction lines are diagonal (i.e., have the same spin-orbital label). For a given pair (α, β) this generates the twelve diagrams shown in Figs. 5 (a)–(l); six of these (a)–(f), arise from the Coulomb integral and six, (g)–(l), from the exchange integral. In addition to these diagram there are twelve other third pert-order diagrams that contribute; these are shown in Figs. 6(a)–(l) and arise from exchanges of appropriate particle or hole lines of the corresponding diagram in Fig. 5.

If we consider the second pert-order Coulomb diagram alone [Fig. 1(a)] and form the infinite series starting with the diagrams in Fig. 7, we obtain

$$\begin{aligned}\sum_{r,s} &\frac{|\langle rs|v|\alpha\beta\rangle|^2}{(\epsilon_\alpha + \epsilon_\beta - \epsilon_r - \epsilon_s)} \\ &\times \left\{1 + \frac{\langle rs|v|rs\rangle}{(\epsilon_\alpha + \epsilon_\beta - \epsilon_r - \epsilon_s)} + \left[\frac{\langle rs|v|rs\rangle}{(\epsilon_\alpha + \epsilon_\beta - \epsilon_r - \epsilon_s)}\right]^2 + \cdots\right\} \\ &= \frac{|\langle rs|v|\alpha\beta\rangle|^2}{(\epsilon_\alpha + \epsilon_\beta - \epsilon_r - \epsilon_s - \langle rs|v|rs\rangle)}\,.\end{aligned} \tag{38}$$

Thus, we have geometrically summed this class of diagrams, called particle ladders, to infinite pert-order. In this series the particle states have been kept diagonal each time a particle line is cut by an interaction line. We refer to this restriction as the *diagonal approximation*. From Eq. (38) we see that this infinite summation in the diagonal approximation is equivalent to a shift of the energy denominator by the direct matrix element between particle states r and s. If we introduce into the series of Eq. (38) the additional diagrams

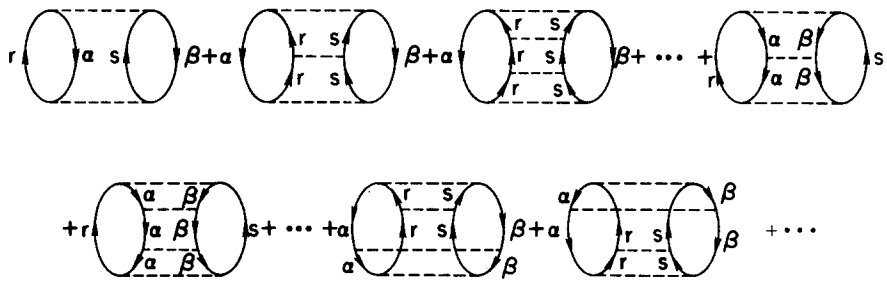

FIG. 8. The particle–particle ladder plus hole–hole ladder geometric series.

corresponding to hole ladders to obtain the series of diagrams shown in Fig. 8, we obtain

$$\sum_{r,s} \frac{|\langle rs|v|\alpha\beta\rangle|^2}{(\epsilon_\alpha+\epsilon_\beta-\epsilon_r-\epsilon_s-\langle rs|v|rs\rangle-\langle\alpha\beta|v|\alpha\beta\rangle} \quad . \tag{39}$$

In Eq. (39) we have summed both the particle and hole ladder diagonal particle pair diagrams to infinite pert-order including all cross terms between them (i.e., diagrams including all possible mixtures of particle–particle and hole–hole interactions). This leads to a shift in the energy denominator by the integrals $\langle rs|v|rs\rangle$ and $\langle\alpha\beta|v|\alpha\beta\rangle$, which are the diagonal particle–particle and hole–hole matrix elements that first appear in the third pert-order diagrams.

If we now generalize this procedure to begin with the Coulomb and exchange diagrams of Fig. 2 and sum both the diagonal particle and diagonal hole ladders to infinite pert-order including all diagrams of Figs. 5 and 6, all corresponding higher pert-order diagrams and all cross terms (i.e., diagrams including all possible mixtures of interactions), we obtain the energy expression in the diagonal approximation,

$$\Delta E^d_{(\alpha\beta)} = \sum_{r,s} \frac{\langle rs|v|\tilde{\alpha\beta}\rangle\langle\alpha\beta|v|rs\rangle}{(\epsilon_\alpha+\epsilon_\beta-\epsilon_r-\epsilon_s+\Delta)} \quad , \tag{40}$$

where Δ is

$$\Delta = -\langle\alpha\beta|v|\tilde{\alpha\beta}\rangle - \langle rs|v|\tilde{rs}\rangle + \langle r\alpha|v|\tilde{r\alpha}\rangle + \langle r\beta|v|\tilde{r\beta}\rangle + \langle s\alpha|v|\tilde{s\alpha}\rangle + \langle s\beta|v|\tilde{s\beta}\rangle \quad . \tag{41}$$

Comparing Eqs. (40) and (41) with the expanded version of Eq. (37), we see that the two are identical. Thus, the solution to Eq. (33) under the approximations of Eq. (34) is equivalent to the second pert-order diagrams plus the geometric sums to infinite pert-order that arise from all the third pert-order diagrams in the diagonal–particle diagonal–hole approximation.

All the diagrams included in Eq. (40) are characterized by having two and only two independent hole lines between each adjacent pair of interaction lines. There cannot be more than two independent hole lines, since we are examining only the second h-order diagrams. If there were only one independent hole line between adjacent interaction lines there would be a cancelling exchange diagram [see Figs. 4(a) and (b)]. Such diagrams do not arise in the configuration interaction expansion because they violate the exclusion principle. Kelly has called the diagrams we summed to obtain Eq. (40) "exclusion principle violating (EPV)" diagrams[5] because they appear to represent simultaneous occupation of a spin-orbital by more than one electron. The term EPV is somewhat misleading in that $\Delta E_{(\alpha\beta)}$ is derivable from a completely antisymmetric wavefunction.

We now examine which additional diagrams appear when $\Delta E_{(\alpha\beta)}$ is not set equal to zero in the denominator of Eq. (33). To find the type of terms that contribute, we expand Eq. (33) subject to the approximation that $\mathbf{D} \cong \mathbf{d}$ and obtain (we use the symbol $\Delta E^r_{(\alpha\beta)}$ for this approximation to the pair energy)

$$\Delta E^r_{(\alpha\beta)} = -\left[\mathbf{B}\frac{1}{\mathbf{d}}\mathbf{B}^+ + \mathbf{B}\frac{1}{\mathbf{d}}\Delta E^r_{(\alpha\beta)}\frac{1}{\mathbf{d}}\mathbf{B}^+ + \mathbf{B}\frac{1}{\mathbf{d}}\Delta E^r_{(\alpha\beta)}\frac{1}{\mathbf{d}}\Delta E^r_{(\alpha\beta)}\frac{1}{\mathbf{d}}\mathbf{B}^+ + \cdots\right] = -\mathbf{B}\frac{1}{\mathbf{d}}\sum_{n=0}^{\infty}\left(\Delta E^r_{(\alpha\beta)}\frac{1}{\mathbf{d}}\right)^n\mathbf{B}^+$$

$$= -\left\{\sum_{r,s}\frac{|\langle\Phi^{rs}_{\alpha\beta}|H|\Phi_0\rangle|^2}{\langle\Phi^{rs}_{\alpha\beta}|H|\Phi^{rs}_{\alpha\beta}\rangle-E_0} + \sum_{r,s}\frac{|\langle\Phi^{rs}_{\alpha\beta}|H|\Phi_0\rangle|^2}{(\langle\Phi^{rs}_{\alpha\beta}|H|\Phi^{rs}_{\alpha\beta}\rangle-E_0)^2}\Delta E^r_{(\alpha\beta)} + \sum_{r,s}\frac{|\langle\Phi^{rs}_{\alpha\beta}|H|\Phi_0\rangle|^2}{(\langle\Phi^{rs}_{\alpha\beta}|H|\Phi^{rs}_{\alpha\beta}\rangle-E_0)^3}(\Delta E^r_{(\alpha\beta)})^2 + \cdots\right\} \quad . \tag{42}$$

The form of Eq. (42), in which the energy $\Delta E^r_{(\alpha\beta)}$ appears on both sides of the equation, makes clear that an iterative solution is required. The lowest pert-order contribution, beyond that of Eq. (37), is seen to be

$$-\sum_{r,s}\frac{|\langle\Phi^{rs}_{\alpha\beta}|H|\Phi_0\rangle|^2}{(\langle\Phi^{rs}_{\alpha\beta}|H|\Phi^{rs}_{\alpha\beta}\rangle-E_0)^2}\Delta E^r_{(\alpha\beta)} \cong -\sum_{r,s}\frac{|\langle\Phi^{rs}_{\alpha\beta}|H|\Phi_0\rangle|^2}{(\langle\Phi^{rs}_{\alpha\beta}|H|\Phi^{rs}_{\alpha\beta}\rangle-E_0)^2}\left\{-\sum_{t,u}\frac{|\langle\Phi^{tu}_{\alpha\beta}|H|\Phi_0\rangle|^2}{(\langle\Phi^{tu}_{\alpha\beta}|H|\Phi^{tu}_{\alpha\beta}\rangle-E_0)}\right\} \tag{43}$$

$$\cong -\sum_{r,s}\frac{\langle rs|v|\tilde{\alpha\beta}\rangle\langle\alpha\beta|v|rs\rangle}{(\epsilon_\alpha+\epsilon_\beta-\epsilon_r-\epsilon_s)^2}\sum_{t,u}\frac{\langle tu|v|\tilde{\alpha\beta}\rangle\langle\alpha\beta|v|tu\rangle}{(\epsilon_\alpha+\epsilon_\beta-\epsilon_t-\epsilon_u)} \quad , \tag{44}$$

where we have taken the lowest pert-order contribution to $\Delta E^r_{(\alpha\beta)}$ and then expanded the denominators to include only orbital energy differences. The two fourth pert-order diagrams that yield the direct contribution to Eq. (43) are shown in Fig. 9. When we add them together, they give

$$-\sum_{rstu}\frac{|\langle rs\,|\,v\,|\,\alpha\beta\rangle|^2\,|\langle ut\,|\,v\,|\,\alpha\beta\rangle|^2}{(\epsilon_\alpha+\epsilon_\beta-\epsilon_r-\epsilon_s)^2(2\epsilon_\alpha+2\epsilon_\beta-\epsilon_r-\epsilon_s-\epsilon_t-\epsilon_u)}-\sum_{rstu}\frac{|\langle rs\,|\,v\,|\,\alpha\beta\rangle|^2\,|\langle ut\,|\,v\,|\,\alpha\beta\rangle|^2}{(\epsilon_\alpha+\epsilon_\beta-\epsilon_r-\epsilon_s)(\epsilon_\alpha+\epsilon_\beta-\epsilon_t-\epsilon_u)(2\epsilon_\alpha+2\epsilon_\beta-\epsilon_r-\epsilon_s-\epsilon_t-\epsilon_u)}$$
$$=-\sum_{rstu}\frac{|\langle rs\,|\,v\,|\,\alpha\beta\rangle|^2\,|\langle ut\,|\,v\,|\,\alpha\beta\rangle|^2}{(\epsilon_\alpha+\epsilon_\beta-\epsilon_r-\epsilon_s)^2(\epsilon_\alpha+\epsilon_\beta-\epsilon_t-\epsilon_u)} \tag{45}$$

in agreement with Eq. (44). All of the fourth pert-order diagrams that contribute to Eq. (44) are shown in Fig. 10. They are referred to as pair rearrangement diagrams.[26,35] If we form a geometric series out of the pair rearrangement diagrams, we shift the denominator of the second pert-order terms by the second pert-order energy. From the direct terms in Fig. 9 and the corresponding higher pert-order terms like Fig. 11(a), we have

$$\sum_{rs}\frac{|\langle rs\,|\,v\,|\,\alpha\beta\rangle|^2}{(\epsilon_\alpha+\epsilon_\beta-\epsilon_r-\epsilon_s+q_{\alpha\beta})}\ , \tag{46}$$

where

$$q_{\alpha\beta}=\sum_{t,u}\frac{|\langle ut\,|\,v\,|\,\alpha\beta\rangle|^2}{(\epsilon_\alpha+\epsilon_\beta-\epsilon_t-\epsilon_u)}\ . \tag{47}$$

In Eq. (46) we have shifted the denominator by the value of the second pert-order diagram. If we now shift the denominator of Eq. (47) by $q_{\alpha\beta}$ and iterate, we obtain an equation of the form

$$Q_{(\alpha\beta)}=\sum_{rs}\frac{|\langle rs\,|\,v\,|\,\alpha\beta\rangle|^2}{(\epsilon_\alpha+\epsilon_\beta-\epsilon_r-\epsilon_s+Q_{(\alpha\beta)})}\ . \tag{48}$$

An example of the additional diagrams included due to the iteration is shown in Fig. 11(b). The same procedure can be carried out for all the diagrams in Fig. 10 and their higher-order counterparts. Furthermore, it is again possible to perform all the diagonal particle–particle, hole–hole, and hole–particle ladder summations on each piece of the rearrangement diagrams. The resulting expression is identical to Eq. (42); that is,

$$\Delta E^{r}_{(\alpha\beta)}=\sum_{r,s}\frac{|\langle rs\,|\,v\,|\,\tilde{\alpha}\beta\rangle\langle\alpha\beta\,|\,v\,|\,rs\rangle}{E_0-\langle\Phi^{rs}_{\alpha\beta}\,|H|\,\Phi^{rs}_{\alpha\beta}\rangle+\Delta E^{r}_{(\alpha\beta)}}\ . \tag{49}$$

We call $\Delta E^{r}_{(\alpha\beta)}$ the "diagonal" pair correlation energy for the pair $(\alpha\beta)$; from the development it is clear that it includes rearrangement contributions.

To relax the approximation ($\mathbf{D}=\mathbf{d}$) made in Eq. (34), we write

$$\mathbf{D}=\mathbf{d}+\mathbf{P}\ . \tag{50}$$

If we retain the approximation $\Delta E_{(\alpha\beta)}=0$ from Eq. (34) to simplify the development, we can write the correlation energy for the pair $(\alpha\beta)$, $\overline{\Delta E}_{(\alpha\beta)}$, as

$$\overline{\Delta E}_{(\alpha\beta)}=-\mathbf{B}(\mathbf{d}+\mathbf{P})^{-1}\mathbf{B}^{+}\ . \tag{51}$$

Expanding the denominator of Eq. (51), we obtain

$$\overline{\Delta E}_{(\alpha\beta)}=-\mathbf{B}\frac{1}{\mathbf{d}}\mathbf{B}^{+}+\mathbf{B}\frac{1}{\mathbf{d}}\mathbf{P}\frac{1}{\mathbf{d}}\mathbf{B}^{+}-\mathbf{B}\frac{1}{\mathbf{d}}\mathbf{P}\frac{1}{\mathbf{d}}\mathbf{P}\frac{1}{\mathbf{d}}\mathbf{B}^{+}+\cdots\ . \tag{52}$$

The first term on the right-hand side of Eq. (52) is the Epstein–Nesbet result $\Delta E^{d}_{(\alpha\beta)}$ of Eq. (37), and the correction terms in Eq. (52) involve the matrix, $\mathbf{P}$. As is evident from its definition, $\mathbf{P}$ contains the nondiagonal particle corrections of the form

$$\langle\Phi^{rs}_{\alpha\beta}\,|H|\,\Phi^{tu}_{\alpha\beta}\rangle=\langle rs\,|\,v\,|\,\tilde{tu}\rangle\ . \tag{53}$$

This matrix element appears in lowest pert-order in the diagrams shown in Fig. 12 and yields the nondiagonal particle–particle ladder contributions to the second term on the right hand side of Eq. (52). They are exactly the particle ladder diagrams summed in Epstein–Nesbet perturbation theory except that the diagonal particle approximation has been relaxed. Thus, to solve for the pair energy making only the approximation, $\Delta E_{(\alpha\beta)}\cong 0$ of Eq. (34), we sum exactly the same type of diagrams that appear in Epstein–Nesbet perturbation theory except that both the diagonal and nondiagonal particle contributions are included. If in addition we introduce the rearrangement diagrams with the nondiagonal particle ladders summed, we obtain the pair energy given in Eq. (33). The sum of these pair terms for every pair of electrons in the system gives the two-body contribution to the correlation energy. This is the complete second h-order energy, E_2, except for the single excitations.

C. The contribution of single excitations to the pair energies

We now consider the pair contributions made by the single excitation diagrams. Brillouin's theorem shows that there is no direct coupling between the ground state and the single excitations for a Hartree–Fock wavefunction. In the pair approximation, the single excitations will affect the energy only by coupling with the double excitations. To analyze the nature of these terms, we use the appropriate matrix form of the Schrödinger equation,

$$\begin{bmatrix}0 & 0 & \mathbf{B}\\ 0 & \mathbf{S} & \mathbf{C}_d\\ \mathbf{B}^{+} & \mathbf{C}_d^{+} & \mathbf{D}\end{bmatrix}\begin{bmatrix}1\\ \mathbf{f}_1\\ \mathbf{f}_2\end{bmatrix}=\Delta E^{s}_{(\alpha\beta)}\begin{bmatrix}1\\ \mathbf{f}_1\\ \mathbf{f}_2\end{bmatrix}\ , \tag{54}$$

where $\Delta E^{s}_{(\alpha\beta)}$ is the pair energy including single excitations, $\mathbf{S}$ contains the matrix elements of the Hamiltonian over the single excitations from one of the orbitals α or β, $\mathbf{C}_d$ contains the matrix elements that couple the single and the double excitations, $\mathbf{f}_1$ is the vector that contains the single-excitation pair CI coefficients, $\mathbf{f}_2$ contains the double-excitation pair CI coefficients; $\mathbf{B}$ and $\mathbf{D}$ are the same matrices as in Eq. (30).

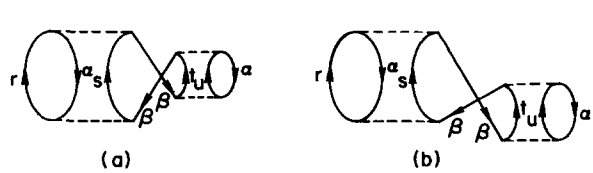

FIG. 9. Two fourth pert-order pair rearrangement diagrams [see Eq. (45)].

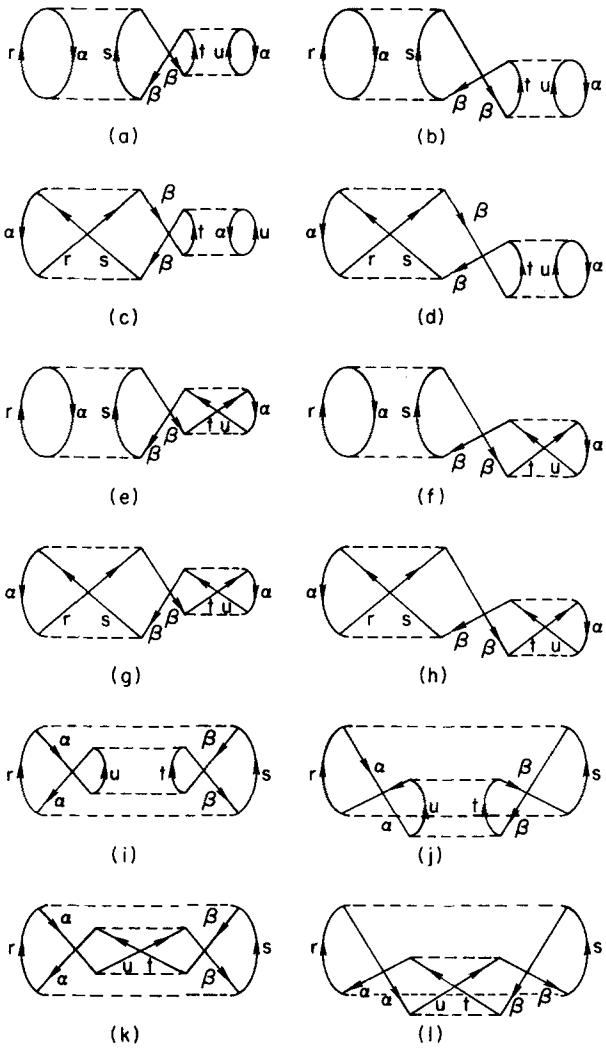

FIG. 10. The lowest (fourth) pert-order pair rearrangement diagrams.

Solving Eq. (54) for $\Delta E^s_{(\alpha\beta)}$, we obtain

$$\Delta E^s_{(\alpha\beta)} = \mathbf{B}\left[\Delta E^s_{(\alpha\beta)}\mathbf{I} - \mathbf{D} - \mathbf{C}_d^+ \frac{1}{\Delta E^s_{(\alpha\beta)}\mathbf{I} - \mathbf{S}} \mathbf{C}_d\right]^{-1} \mathbf{B}^+ , \tag{55}$$

which yields upon expansion

$$\Delta E^s_{(\alpha\beta)} = \mathbf{B}\frac{1}{\Delta E^s_{(\alpha\beta)}\mathbf{I} - \mathbf{D}}\mathbf{B}^+ + \mathbf{B}\frac{1}{\Delta E^s_{(\alpha\beta)}\mathbf{I} - \mathbf{D}}\mathbf{C}_d^+\frac{1}{\Delta E^s_{(\alpha\beta)}\mathbf{I} - \mathbf{S}} \times \mathbf{C}_d\frac{1}{\Delta E^s_{(\alpha\beta)}\mathbf{I} - \mathbf{D}}\mathbf{B}^+ + \cdots . \tag{56}$$

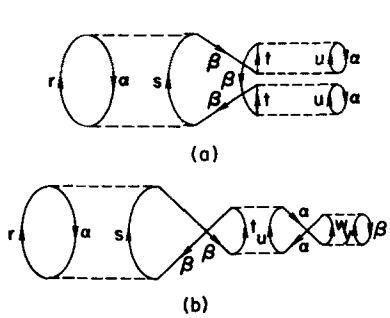

FIG. 11. Pair rearrangement diagrams that contribute to (a) geometric series [Eq. (46)] and (b) the iterated geometric series [Eq. (46)].

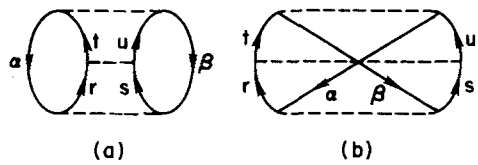

FIG. 12. Lowest pert-order nondiagonal particle pair ladder diagrams.

The effect of the single excitations appears in $\Delta E^s_{(\alpha\beta)}$ of the first term and in the second and subsequent terms on the right hand side of Eq. (56). We consider first the result obtained with the approximations that $\Delta E^s_{(\alpha\beta)} \cong 0$ and **D** and **S** are diagonal. In the diagonal approximation, the matrix elements of **S** are given by

$$E_0 - \langle \Phi^r_\alpha | H | \Phi^r_\alpha \rangle = \epsilon_\alpha - \epsilon_r + \langle r\alpha | v | \tilde{r\alpha} \rangle . \tag{57}$$

The matrix elements of $\mathbf{C}_d$ have the form

$$\langle \Phi^r_\alpha | H | \Phi^{rs}_{\alpha\beta} \rangle = \langle r\beta | v | \tilde{rs} \rangle - \langle \beta\alpha | v | \tilde{s\alpha} \rangle . \tag{58}$$

The second term on the right hand side of Eq. (56) consists of products of two **B** matrix elements times two $\mathbf{C}_d$ matrix elements divided by two double excitation energy denominators and one single excitation energy denominator. Because of the form of this term, the four matrix elements in the numerator and three energy denominators, the lowest pert-order singles–doubles coupling diagrams appear in fourth pert-order. This suggests that the single excitation contributions are small and partially justifies their neglect relative to double excitations in calculations of the energy for closed-shell systems. A more extensive discussion of the terms in the CI expansion and the lowest pert-orders in which they occur can be found in Reference 34. The direct contributions are of the form shown in Fig. 13, where the non-diagonal form of the diagrams is given. In analogy with the double excitation case, the full solution to Eq. (55) is obtained by starting with these low pert-order diagrams and performing infinite ladder and rearrangement summations with the restriction to no more than two independent hole lines in all of the diagrams. We note that for open-shell systems in the restricted Hartree–Fock approximation, the single excitations can couple directly to the ground state and are expected to be more important than in the closed-shell case (see Sec. IV, H_3).

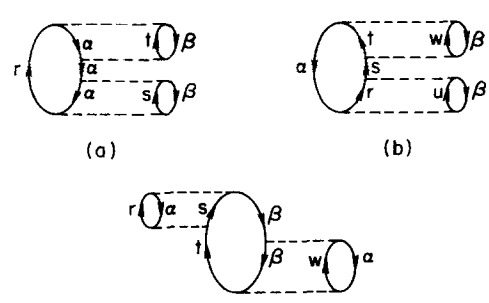

FIG. 13. The lowest pert-order direct single excitation pair diagrams.

D. Pair coupling terms; relation to double excitation configuration interaction

In the two previous subsections we expressed the correlation energy in terms of the cluster expansion of Eq. (22) and determined which terms to sum to obtain the two-body effects. In this section we wish to briefly examine the higher h-order corrections and then use the present formulation for an analysis of double excitation configuration interaction treatments.

Equation (22) implies that we should next sum all diagrams with three independent hole lines. The diagrams with three independent hole lines are of three distinct types:

(1) third and higher pert-order diagrams that have no more than two hole lines occurring between any two adjacent interaction lines;

(2) rearrangement diagrams with three independent hole lines; and

(3) higher pert-order diagrams that have more than two hole lines between a pair of adjacent interaction lines.

Figure 14(a) shows an example of type 1, 14(b) an example of type 2, and 14(c) shows an example of type 3. The diagrams of types 1 and 2 arise from the double-excited determinants in the configuration interaction expansion, and the terms of type 3 involve triple and higher excitations. Terms, other than the pair terms already discussed, that appear in the doubly excited part of the configuration interaction expansion are referred to as "pair coupling" terms. They occur in all h-orders and all pert-orders. Diagrammatically, the pair coupling terms are of three types:

(1) higher h-order ($h \geq 3$) diagrams with no more than two independent hole lines occurring between any adjacent pair of interaction lines [diagrams 14(a) and 14(d)];

(2) pair coupling rearrangement diagrams (with $h \geq 3$) [diagrams 14(b) and 14(e)]; and

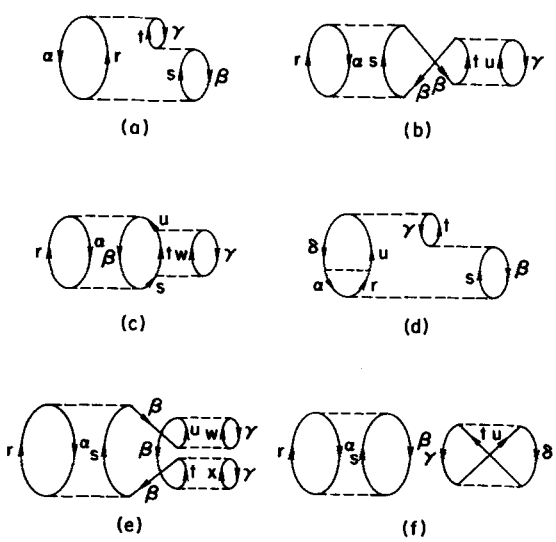

FIG. 14. Higher hole-order diagrams (see text).

(3) unlinked pair coupling diagrams [diagram 14(f)].

To determine in what way the three types of pair coupling diagrams appear in a CI calculation consisting of all double excitations, we proceed as we did in our analysis of the pair contributions, all of which are included. We ignore single excitations for simplicity, their inclusion requiring a simple extension of the arguments for the pair single excitation diagrams. We focus first on the coupling terms between two particular distinct pairs; the coupling terms between all the other distinct pairs in the system can be treated in the same way. Then, we consider the diagrams that appear if the pairs are not distinct; i.e., if any of the hole or particle states involved in the two pairs are the same.

The configuration interaction matrix for two pairs, $1(\alpha\beta)$ and $2(\gamma\delta)$, neglecting single excitations, is

$$\begin{bmatrix} 0 & \mathbf{B}_1 & \mathbf{B}_2 \\ \mathbf{B}_1^\dagger & \mathbf{D}_1 & \mathbf{C}_{12} \\ \mathbf{B}_2^\dagger & \mathbf{C}_{12}^\dagger & \mathbf{D}_2 \end{bmatrix} .$$

in an obvious extension of the notation used in Eq. (30); the pair coupling matrix is $\mathbf{C}_{12}$. In pair theory we approximate the lowest eigenvalue of this matrix by the sum of the lowest eigenvalues of the matrices

$$\begin{bmatrix} 0 & \mathbf{B}_1 \\ \mathbf{B}_1^\dagger & \mathbf{D}_1 \end{bmatrix} , \quad \begin{bmatrix} 0 & \mathbf{B}_2 \\ \mathbf{B}_2^\dagger & \mathbf{D}_2 \end{bmatrix} .$$

The pair coupling terms arise both from diagonalizing the full matrix (in the absence of coupling terms; $\mathbf{C}_{12} = 0$)

$$\begin{bmatrix} 0 & \mathbf{B}_1 & \mathbf{B}_2 \\ \mathbf{B}_1^\dagger & \mathbf{D}_1 & 0 \\ \mathbf{B}_2^\dagger & 0 & \mathbf{D}_2 \end{bmatrix} ,$$

and from the coupling matrix $\mathbf{C}_{12}$.

To analyze the pair coupling terms we first consider the matrix in the approximation that $\mathbf{C}_{12} = 0$. The lowest eigenvalue of this matrix, ΔE_{CR}, is obtained by solving the secular equation

$$\begin{bmatrix} 0 & \mathbf{B}_1 & \mathbf{B}_2 \\ \mathbf{B}_1^\dagger & \mathbf{D}_1 & 0 \\ \mathbf{B}_2^\dagger & 0 & \mathbf{D}_2 \end{bmatrix} \begin{bmatrix} 1 \\ \mathbf{f}_1 \\ \mathbf{f}_2 \end{bmatrix} = \Delta E_{CR} \begin{bmatrix} 1 \\ \mathbf{f}_1 \\ \mathbf{f}_2 \end{bmatrix} . \tag{59}$$

The resulting value of ΔE_{CR} is

$$\Delta E_{CR} = \mathbf{B}_1 \frac{1}{\Delta E_{CR}\mathbf{I} - \mathbf{D}_1} \mathbf{B}_1^\dagger + \mathbf{B}_2 \frac{1}{\Delta E_{CR}\mathbf{I} - \mathbf{D}_2} \mathbf{B}_2^\dagger . \tag{60}$$

This is to be compared with the pair expression for this case [see Eq. (33)],

$$\Delta E_{(\alpha\beta)} + \Delta E_{(\gamma\delta)} = \mathbf{B}_1 \frac{1}{\Delta E_1 \mathbf{I} - \mathbf{D}_1} \mathbf{B}_1^\dagger + \mathbf{B}_2 \frac{1}{\Delta E_2 \mathbf{I} - \mathbf{D}_2} \mathbf{B}_2^\dagger , \tag{61}$$

where ΔE_1 is the pair energy of pair 1 and ΔE_2 is that

of pair 2. For this case of distinct pairs, the additional diagrams summed in Eq. (60) but not included in Eq. (61) are unlinked diagrams. To demonstrate this, we simplify the expressions by making the diagonal approximation [Eq. (49)] in Eq. (60). Writing ΔE_{CR} in this approximation as ΔE^d_{CR}, we have

$$\Delta E^d_{CR} = \sum_{rs} \frac{\langle rs \mid v \mid \tilde{\alpha\beta}\rangle\langle \alpha\beta \mid v \mid rs\rangle}{E_0 - \langle \Phi^{rs}_{\alpha\beta} \mid H \mid \Phi^{rs}_{\alpha\beta}\rangle + \Delta E^d_{CR}} + \sum_{tu} \frac{\langle tu \mid v \mid \tilde{\gamma\delta}\rangle\langle \gamma\delta \mid v \mid tu\rangle}{E_0 - \langle \Phi^{tu}_{\gamma\delta} \mid H \mid \Phi^{tu}_{\gamma\delta}\rangle + \Delta E^d_{CR}} \quad , \tag{62}$$

where the sums on r, s and t, u are restricted so that we include only excitations out of the two distinct pairs (α, β) and (γ, δ) $(\alpha \neq \beta \neq \gamma \neq \delta)$ into the distinct particle states (r, s) and (t, u) $(r \neq s \neq t \neq u)$. Approximating the differences in determinantal energies by the differences in orbital energies, we obtain

$$\overline{\Delta E}_{CR} = \sum_{rs} \frac{\langle rs \mid v \mid \tilde{\alpha\beta}\rangle\langle \alpha\beta \mid v \mid rs\rangle}{(\epsilon_\alpha + \epsilon_\beta - \epsilon_r - \epsilon_s + \overline{\Delta E}_{CR})} + \sum_{tu} \frac{\langle tu \mid v \mid \tilde{\gamma\delta}\rangle\langle \gamma\delta \mid v \mid tu\rangle}{(\epsilon_\gamma + \epsilon_\delta - \epsilon_t - \epsilon_u + \overline{\Delta E}_{CR})} \quad . \tag{63}$$

Expanding $\overline{\Delta E}_{CR}$ on the right hand side of Eq. (63), we find

$$\overline{\Delta E}_{CR} = \sum_{rs} \frac{\langle rs \mid v \mid \tilde{\alpha\beta}\rangle\langle \alpha\beta \mid v \mid rs\rangle}{(\epsilon_\alpha + \epsilon_\beta - \epsilon_r - \epsilon_s)} \left[1 - \frac{\overline{\Delta E}_{CR}}{(\epsilon_\alpha + \epsilon_\beta - \epsilon_r - \epsilon_s)} + \cdots\right] + \sum_{tu} \frac{\langle tu \mid v \mid \tilde{\gamma\delta}\rangle\langle \gamma\delta \mid v \mid tu\rangle}{(\epsilon_\gamma + \epsilon_\delta - \epsilon_t - \epsilon_u)} \left[1 - \frac{\overline{\Delta E}_{CR}}{(\epsilon_\gamma + \epsilon_\delta - \epsilon_t - \epsilon_u)} + \cdots\right] . \tag{64}$$

The first terms on the right hand side of Eq. (64) which contain a $\overline{\Delta E}_{CR}$ contribution have the lowest pert-order contributions to Eq. (63) that are unlinked; e.g., the expression

$$A = -\sum_{rs} \frac{\langle rs \mid v \mid \tilde{\alpha\beta}\rangle\langle \alpha\beta \mid v \mid rs\rangle}{(\epsilon_\alpha + \epsilon_\beta - \epsilon_r - \epsilon_s)} \left[\frac{\overline{\Delta E}_{CR}}{(\epsilon_\alpha + \epsilon_\beta - \epsilon_r - \epsilon_s)}\right] \tag{65}$$

contains unlinked terms. To see this, we approximate $\overline{\Delta E}_{CR}$ by its lowest-order contribution

$$\overline{\Delta E}_{CR} \cong \sum_{rs} \frac{\langle rs \mid v \mid \tilde{\alpha\beta}\rangle\langle \alpha\beta \mid v \mid rs\rangle}{(\epsilon_\alpha + \epsilon_\beta - \epsilon_r - \epsilon_s)} + \sum_{tu} \frac{\langle tu \mid v \mid \tilde{\gamma\delta}\rangle\langle \gamma\delta \mid v \mid tu\rangle}{(\epsilon_\gamma + \epsilon_\delta - \epsilon_t - \epsilon_u)} \quad . \tag{66}$$

The first sum of Eq. (66) gives the pair rearrangement contribution considered in Eqs. (42)–(49). The second sum, when introduced into Eq. (65), leads to a product of the form

$$\sum_{rs} \frac{\langle rs \mid v \mid \tilde{\alpha\beta}\rangle\langle \alpha\beta \mid v \mid rs\rangle}{(\epsilon_\alpha + \epsilon_\beta - \epsilon_r - \epsilon_s)^2} \sum_{tu} \frac{\langle tu \mid v \mid \tilde{\gamma\delta}\rangle\langle \gamma\delta \mid v \mid tu\rangle}{(\epsilon_\gamma + \epsilon_\delta - \epsilon_t - \epsilon_u)} . \tag{67}$$

Equation (67) corresponds to the sum of the unlinked diagrams shown in Figs. 15(a) and 15(b), which represent the lowest pert-order contributions to the energy denominator shift in Eq. (63). To obtain the full denominator shift, $\overline{\Delta E}_{CR}$, an iterative equation must be solved. The formal structure of this equation is exactly the same as Eq. (42). In analogy with the pair rearrangement diagram case, the coupling correction [Eq. (63)] is obtained by summing geometrically the unlinked diagrams of the type shown in Figs. 15(a), (b), and (c), and iteratively summing the diagrams of the type shown in Fig. 15(d). To obtain the complete

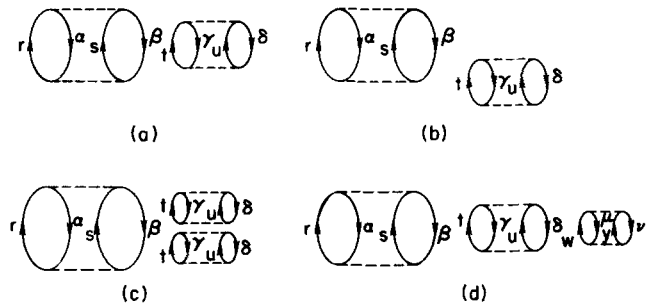

FIG. 15. Unlinked pair-coupling diagrams (see text).

diagonal energy ΔE^d_{CR} [Eq. (62)], we must for each unlinked part of all the diagrams summed in Eq. (63) sum all the diagonal particle–particle, diagonal particle–hole, and diagonal hole–hole diagrams that were summed in deriving the Epstein–Nesbet perturbation formula. Similarly, for Eq. (60) we sum the same diagrams as those summed in Eq. (62) without the diagonal approximation.

In determining the diagrams included in Eq. (63) [and Eq. (60) and Eq. (62)], we have assumed that pair 1 and 2 are distinct; i.e., pair 1 and pair 2 do not have any orbital (particle or hole) in common. We now examine the coupling terms arising from the interaction between pairs where one occupied orbital in each pair is the same; in the CI expansion, this corresponds to excitations involving determinants of the form $|\Phi^{rs}_{\alpha\beta}\rangle$ and $|\Phi^{tu}_{\alpha\gamma}\rangle$. If we make the same approximation to Eq. (60) as was made to obtain Eq. (63), we find

$$\overline{\Delta E}_{CR} = \sum_{rs} \frac{\langle rs \mid v \mid \tilde{\alpha\beta}\rangle\langle \alpha\beta \mid v \mid rs\rangle}{(\epsilon_\alpha + \epsilon_\beta - \epsilon_r - \epsilon_s + \overline{\Delta E}_{CR})} + \sum_{tu} \frac{\langle tu \mid v \mid \tilde{\alpha\gamma}\rangle\langle \alpha\gamma \mid v \mid tu\rangle}{(\epsilon_\alpha + \epsilon_\gamma - \epsilon_t - \epsilon_u + \overline{\Delta E}_{CR})} \quad . \tag{68}$$

When we expand $\overline{\Delta E}_{CR}$ in the denominator of Eq. (68) and keep only the lowest order terms we have contributions of the form

$$A \cong -\sum_{rs} \frac{\langle rs \mid v \mid \tilde{\alpha\beta}\rangle\langle \alpha\beta \mid v \mid rs\rangle}{(\epsilon_\alpha + \epsilon_\beta - \epsilon_r - \epsilon_s)} \sum_{tu} \frac{\langle tu \mid v \mid \tilde{\alpha\gamma}\rangle\langle \alpha\gamma \mid v \mid tu\rangle}{(\epsilon_\alpha + \epsilon_\gamma - \epsilon_t - \epsilon_u)} . \tag{69}$$

Equation (69) is obtained by summing the diagrams like those in Figs. 16(a) and 16(b). Unlike the interaction between two pairs with no orbitals in common (Fig. 15), the contributions in this case are linked. The diagrams in Figs. 16(a) and 16(b) are called coupling rearrangement diagrams and they are the coupling terms discussed by Kelly.[26] In analogy with the unlinked situation, the denominator shift of Eq. (68) is found by summing coupling rearrangement diagrams like those of Figs. 16(a), (b), and (c) geometrically and iterating with diagrams like that of Fig. 16(d). Similarly, for Eq. (60) or Eq. (62), we must perform the appropriate ladder summations. Linked diagrams also arise when the excitations from both pairs involve the same particle state; i.e.,

$$\overline{\Delta E}_{CR} = \sum_r \left\{ \sum_s \frac{\langle rs \mid v \mid \tilde{\alpha\beta}\rangle\langle \alpha\beta \mid v \mid rs\rangle}{\epsilon_\alpha + \epsilon_\beta - \epsilon_r - \epsilon_s + \overline{\Delta E}_{CR}} \right.$$

$$+\sum_t \frac{\langle rt|v|\tilde{\gamma}\delta\rangle\langle\gamma\delta|v|rt\rangle}{\epsilon_\gamma+\epsilon_\delta-\epsilon_r-\epsilon_t+\Delta\bar{E}_{CR}}\Bigg\} \tag{70}$$

whose lowest-order coupled contribution is of the type shown in Fig. 16(e).

We have seen that the solution for the energy in Eq. (59) is given by the pair contributions, coupling rearrangement diagrams when any of the hole or particle label of a coupled pair are the same, and unlinked diagrams. As Goldstone has shown unlinked diagrams do not contribute to the correlation energy.[28] To resolve this apparent inconsistency between the Goldstone expansion and the CI expansion we show in the appendix that the unlinked terms in Eq. (63) are canceled when we include quadruple excitations in the CI expansion.

To find the remaining diagrams included in the double excitation CI treatment, we now examine the effect of the pair coupling matrix elements in the block $\mathbf{C}_{12}$; that is, we consider the equation

$$\begin{bmatrix} 0 & \mathbf{B}_1 & \mathbf{B}_2 \\ \mathbf{B}_1^\dagger & \mathbf{D}_1 & \mathbf{C}_{12} \\ \mathbf{B}_2^\dagger & \mathbf{C}_{12}^\dagger & \mathbf{D}_2 \end{bmatrix} \begin{bmatrix} 1 \\ \mathbf{f}_1 \\ \mathbf{f}_2 \end{bmatrix} = \Delta E_d \begin{bmatrix} 1 \\ \mathbf{f}_1 \\ \mathbf{f}_2 \end{bmatrix} . \tag{71}$$

Solving Eq. (71) for $\mathbf{f}_1$ and $\mathbf{f}_2$, we have

$$\mathbf{f}_1 = \frac{1}{\Delta E_d \mathbf{I}-\mathbf{D}_1}\mathbf{B}_1^\dagger + \frac{1}{\Delta E_d \mathbf{I}-\mathbf{D}_1}\mathbf{C}_{12}\mathbf{f}_2 \tag{72}$$

$$\mathbf{f}_2 = \frac{1}{\Delta E_d \mathbf{I}-\mathbf{D}_2}\mathbf{B}_2^\dagger + \frac{1}{\Delta E_d \mathbf{I}-\mathbf{D}_2}\mathbf{C}_{12}^\dagger\mathbf{f}_1 . \tag{73}$$

Solving simultaneously for ΔE_d, we obtain

$$\begin{aligned}\Delta E_d = {} & \mathbf{B}_1 \frac{1}{\mathbf{I}-\frac{1}{\Delta E_d \mathbf{I}-\mathbf{D}_1}\mathbf{C}_{12}\frac{1}{\Delta E_d \mathbf{I}-\mathbf{D}_2}\mathbf{C}_{12}^\dagger}\frac{1}{\Delta E_d \mathbf{I}-\mathbf{D}_1}\mathbf{B}_1^\dagger + \mathbf{B}_2 \frac{1}{\mathbf{I}-\frac{1}{\Delta E_d \mathbf{I}-\mathbf{D}_2}\mathbf{C}_{12}^\dagger\frac{1}{\Delta E_d \mathbf{I}-\mathbf{D}_1}\mathbf{C}_{12}}\frac{1}{\Delta E_d \mathbf{I}-\mathbf{D}_2}\mathbf{B}_2^\dagger \\ & + \mathbf{B}_1 \frac{1}{\mathbf{I}-\frac{1}{\Delta E_d \mathbf{I}-\mathbf{D}_1}\mathbf{C}_{12}\frac{1}{\Delta E_d \mathbf{I}-\mathbf{D}_2}\mathbf{C}_{12}^\dagger}\frac{1}{\Delta E_d \mathbf{I}-\mathbf{D}_1}\mathbf{C}_{12}\frac{1}{\Delta E_d \mathbf{I}-\mathbf{D}_2}\mathbf{B}_2^\dagger \\ & + \mathbf{B}_2 \frac{1}{\mathbf{I}-\frac{1}{\Delta E_d \mathbf{I}-\mathbf{D}_2}\mathbf{C}_{12}^\dagger\frac{1}{\Delta E_d \mathbf{I}-\mathbf{D}_1}\mathbf{C}_{12}}\frac{1}{\Delta E_d \mathbf{I}-\mathbf{D}_2}\mathbf{C}_{12}^\dagger\frac{1}{\Delta E_d \mathbf{I}-\mathbf{D}_1}\mathbf{B}_1^\dagger .\end{aligned} \tag{74}$$

Expanding the denominators, we have

$$\begin{aligned}\Delta E_d = {} & \mathbf{B}_1\frac{1}{\Delta E_d \mathbf{I}-\mathbf{D}_1}\mathbf{B}_1^\dagger + \mathbf{B}_2\frac{1}{\Delta E_d \mathbf{I}-\mathbf{D}_2}\mathbf{B}_2^\dagger + \mathbf{B}_1\frac{1}{\Delta E_d \mathbf{I}-\mathbf{D}_1}\mathbf{C}_{12}\frac{1}{\Delta E_d \mathbf{I}-\mathbf{D}_2}\mathbf{B}_2^\dagger + \mathbf{B}_2\frac{1}{\Delta E_d \mathbf{I}-\mathbf{D}_2}\mathbf{C}_{12}^\dagger\frac{1}{\Delta E_d \mathbf{I}-\mathbf{D}_1}\mathbf{B}_1^\dagger \\ & + \mathbf{B}_1\frac{1}{\Delta E_d \mathbf{I}-\mathbf{D}_1}\mathbf{C}_{12}\frac{1}{\Delta E_d \mathbf{I}-\mathbf{D}_2}\mathbf{C}_{12}^\dagger\frac{1}{\Delta E_d \mathbf{I}-\mathbf{D}_1}\mathbf{B}_1^\dagger + \mathbf{B}_2\frac{1}{\Delta E_d \mathbf{I}-\mathbf{D}_2}\mathbf{C}_{12}^\dagger\frac{1}{\Delta E_d \mathbf{I}-\mathbf{D}_1}\mathbf{C}_{12}\frac{1}{\Delta E_d \mathbf{I}-\mathbf{D}_2}\mathbf{B}_2^\dagger + \cdots .\end{aligned} \tag{75}$$

If we approximate ΔE_d by ΔE_{CR}, the first two terms on the right-hand side of Eq. (75) give Eq. (60), and the subsequent terms in Eq. (75) contain the effect of the coupling matrix, $\mathbf{C}_{12}$.

To analyze the latter terms, we consider, as an example, the third term on the right-hand side of Eq. (75),

$$\mathbf{B}_1\frac{1}{\Delta E_d \mathbf{I}-\mathbf{D}_1}\mathbf{C}_{12}\frac{1}{\Delta E_d \mathbf{I}-\mathbf{D}_2}\mathbf{B}_2^\dagger . \tag{76}$$

To simplify the argument, we neglect the ΔE_d terms in the denominators, replace the $\mathbf{D}$ matrices by the differences in orbital energies and focus on the coupling between the two determinants $|\Phi_{\alpha\beta}^{rs}\rangle$ and $|\Phi_{\gamma\delta}^{rs}\rangle$ where $\alpha\neq\beta\neq\gamma\neq\delta$. The appropriate element of the matrix $\mathbf{C}_{12}$ is given by

$$\langle\Phi_{\alpha\beta}^{rs}|H|\Phi_{\gamma\delta}^{rs}\rangle = \langle\alpha\beta|v|\tilde{\gamma}\delta\rangle \tag{77}$$

and the corresponding term in Eq. (76) has the form

$$\frac{\langle rs|v|\tilde{\alpha}\beta\rangle\langle\alpha\beta|v|\tilde{\gamma}\delta\rangle\langle\gamma\delta|v|rs\rangle}{(\epsilon_\alpha+\epsilon_\beta-\epsilon_r-\epsilon_s)(\epsilon_\gamma+\epsilon_\delta-\epsilon_r-\epsilon_s)} . \tag{78}$$

This type of term gives the lowest pert-order contribution and couples the two determinants $|\Phi_{\alpha\beta}^{rs}\rangle$ and $|\Phi_{\gamma\delta}^{rs}\rangle$; the contribution of Eq. (78) is shown diagrammatically in Fig. 17. It is clear that this diagram has the same form as the hole ladder diagrams summed in pair theory except that nondiagonal hole labelings appear here. If we continue this analysis by considering other possible coupling terms in $\mathbf{C}_{12}$ we find all possible dia-

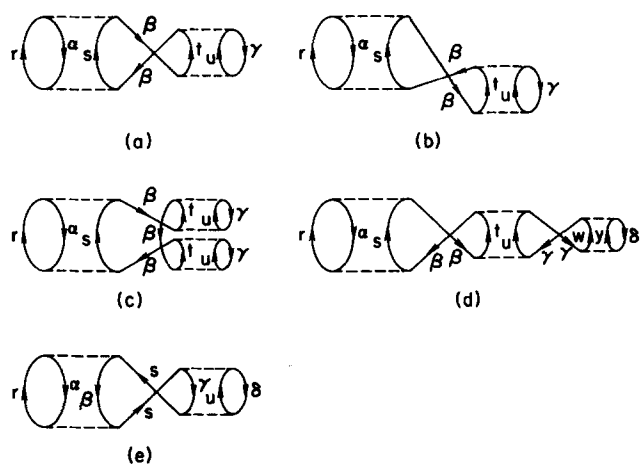

FIG. 16. Linked pair-coupling rearrangement diagrams.

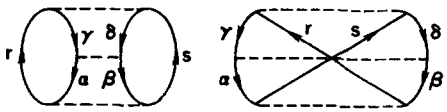

FIG. 17. Hole-hole ladder pair coupling diagrams (see text).

grams of pair structure with the diagonal hole restriction removed. It is important to remember that even when the direct coupling between two pair terms of the type considered here vanishes, there are indirect pair coupling contributions of the type considered in Eq. (60); e.g., for the determinants $|\Phi^{rs}_{\alpha\beta}\rangle$ and $|\Phi^{tu}_{\alpha\gamma}\rangle$; the element of $\mathbf{C}_{12}$,

$$\langle\Phi^{rs}_{\alpha\beta}|H|\Phi^{tu}_{\alpha\gamma}\rangle = 0 \tag{79}$$

but they are indirectly coupled by the rearrangement diagrams.

E. Comparison with other formulations

We have analyzed the electron correlation problem and determined the pair and pair coupling contributions. The tools for this analysis are Goldstone diagrams and matrix partitioning techniques, starting with the cluster expansion defined in terms of hole lines by Eq. (22). This cluster expansion is equivalent to Nesbet's "Heirarchy of Bethe–Goldstone Equations." The first term is the pair theory term, for which we have determined the contributing Goldstone diagrams. Sinanoğlu includes the same pair terms, except for single excitation effects, in the decoupled form of his many-electron theory.[30,31] Kelly evaluated the pair terms by approximating them perturbatively; i.e., he summed the terms in Eq. (49), which is the diagonal approximation to pair theory. Like Sinanoğlu, Kelly did not consider the single excitation effects summed in Eq. (55). Of all the higher hole-order contributions, the pair coupling terms arise in lowest pert-order and in lowest order in the configuration interaction expansion. As a consequence, the pair coupling terms are expected to be the next most important terms after pair theory. In Nesbet's formulation, it is necessary to sum all h-orders to obtain the complete pair-coupling contribution. Other formulations of the correlation problem are able to include these terms in a more systematic way. For example, Kelly, using diagrammatic perturbation theory, evaluates the pair coupling terms by summing the third pert-order three-body diagrams and the coupling rearrangement diagrams.[36] Čižek, Paldus, and Shavitt sum all the pair coupling terms (excluding the unlinked contributions) in "coupled pair many-electron theory".[6,32]

TABLE I. Small basis set for Li_2.[a]

Orbital	Exponent
$1s_\sigma$	2.6894
$2s_\sigma$	0.6335
$2p_\sigma$	0.7609
$E_{HF} = -14.8421$ a.u.	

[a]The internuclear distance is 5.25 a.u.

TABLE II. Correlation energy of Li_2 in the small basis set.[a]

ϵ_2	−0.00573
ϵ_3	−0.00267
$\epsilon_2 + \epsilon_3$	−0.00840
$\Delta E^d_{(\alpha\beta)}$ [Eq. (40)]	−0.001299
$\sum_{\alpha\beta} \Delta E^r_{(\alpha\beta)}$ [Eq. (49)]	−0.01229
$\sum_{\alpha\beta} \Delta E_{(\alpha\beta)}$ [Eq. (33)]	−0.01096
CI doubles only	−0.01100
CI singles and doubles	−0.01154
Full CI	−0.01156

[a]Energies in atomic units; the internuclear distance is 5.25 a.u.

A logical extension of the present development would be to include higher excitations and determine the contributing diagrams. This has been done for quadruple excitations in order to analyze the terms included by Čižek and Paldus in coupled pair many-electron theory.[37] The arguments and techniques for the higher excitations are the same as used in the present paper and it does not appear worthwhile to present the details.

IV. THE CORRELATION ENERGY OF Li_2, N_2, and H_3

In this section we present the results of correlation energy calculations on Li_2, N_2, and H_3. Our primary aim in these calculations is to illustrate the analysis of the many-body methods given in the previous section. With this in mind, we have performed several of these calculations with small basis sets so that a full CI energy could be determined for comparison. In the remaining calculations, we used larger basis sets for which a comparison with experiment would be meaningful. We first examine Li_2 with a six orbital basis set and H_3 with a fifteen orbital basis set; for both of these, comparison with a complete CI calculation is possible. We then present larger basis set results for Li_2 and N_2.

A. Comparison with complete CI calculations

Li_2 molecule

The lithium molecule calculations were performed at an internuclear separation of 5.25 a.u., which is the Hartree–Fock minimum. The basis set consisted of a $1s$-orbital, a $2s$-orbital, and a $2p_\sigma$-orbital on each center; the Slater orbital exponents for these orbitals were taken from Fraga and Ransil[38] and are given in Table I with the Hartree–Fock energy, E_{HF}, for the basis set. We present in Table II a comparison of the correlation contributions given by pert-order Rayleigh–Schrödinger perturbation theory (ϵ_2, ϵ_3), Epstein–Nesbet perturbation theory ($\Delta E^d_{(\alpha\beta)}$), "diagonal" pair theory, total pair theory, and CI at various levels of excitation. It is clear that the Rayleigh–Schrödinger expansion (ϵ_2, ϵ_3, $\epsilon_2+\epsilon_3$) converges rather slowly; this appears to be a general result. By contrast, the $\Delta E^d_{(\alpha\beta)}$

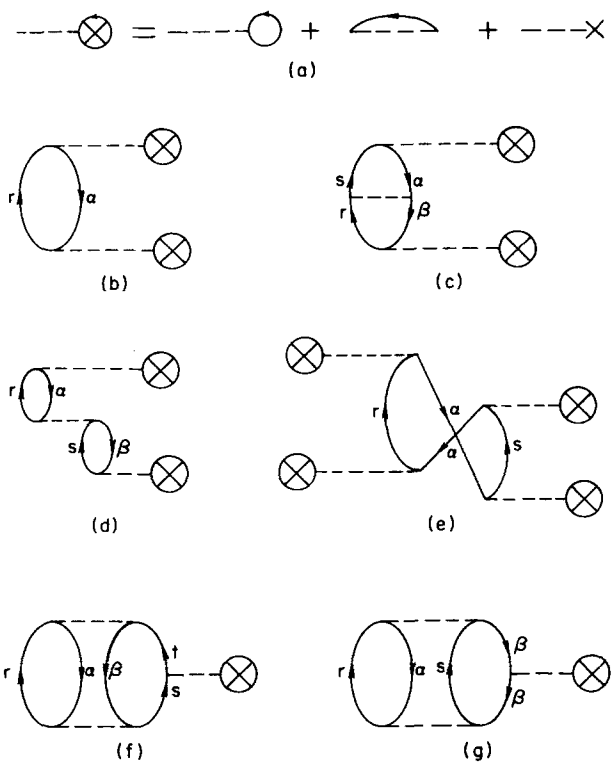

FIG. 18. Core polarization operator and diagrams for the open shell case (see text).

value compares favorably with the CI correlation energy, as do the full pair energies and the diagonal approximation pair energies. Because of the small basis set, only the $(2\sigma_g^+, 2\sigma_g^-)$ pair energy is important; both the inner-shell and intershell pair energies are negligible. It is also evident from the table, that double excitation CI is a very good approximation and that single excitations make a small contribution for this case. The significance of these results has to be regarded with some degree of caution because the total correlation energy for the basis set is only about 10% of the "experimental" correlation energy (see Sec. IV B and Table VI).

H_3 system

For the H_3 system, we consider the saddle point geometry and use the extended Slater basis with optimized exponents employed in the full CI calculation of Shavitt, Stevens, Minn, and Karplus[39] (see Table III). This basis set yields an energy that is estimated to be within ~5 kcal of the true system energy. Since H_3 is an open-shell system and a restricted Hartree–Fock function is being used as $|\Phi_0\rangle$, Brillouin's theorem does not hold; i.e., there are single excitations that couple directly with the ground state. This leads to additional diagrams[37,40] involving the core polarization operator shown in Fig. 18(a); it is nonzero for open-shell systems where the core electrons are restricted to doubly occupy the core orbitals. The resulting diagrams, such as those given in Figs. 18(b)–18(c), are called core polarization diagrams, and we define ΔE_{cp} to be the sum of all such diagrams. The contribution to ΔE_{cp} include the bare diagram shown in Fig. 18(b), its ladder corrections shown in Figs. 18(c) and 18(d), and its rearrangement corrections shown in Fig. 18(e). As with the pair energies, if we only include the diagonal contributions to diagrams 18(c) and 18(d), we obtain the diagonal approximation to the core polarization terms, which we denote by ΔE_{cp}^d. The nonzero value for the core polarization operator also leads to additional pair diagrams of the type shown in Figs. 18(f) and 18(g). These are third pert-order contributions that can be summed to infinite pert order. In Table IV we give the various approximations to the core polarization and the pair contributions obtained for the H_3 system at the saddle point; also included are the results of a configuration interaction calculation including only single and double excited configurations and including all configurations.[39] The full core polarization correction, ΔE_{cp} was computed by diagonalizing the CI matrix truncated at single excitations, while ΔE_{cp}^d was obtained by diagram summation. The core polarization terms contribute approximately 35% of the total correlation energy associated with the basis set; the diagonal contribution is seen to yield about 95% of the total. In Table IV, we also compare two approximations [Eqs. (40) and (49)] to the pair energy [Eq. (33)]; in all cases

TABLE III. Basis set for linear symmetric H_3.[a]

Orbital	Center	Exponent
$1s$	1, 2	0.860
$1s'$	1, 2	1.210
$1s$	3	0.967
$1s'$	3	1.215
$2p$	1, 2	1.572
$2p$	3	1.640

$E_{HF} = -1.594248$ a.u.

[a]Centers 1 and 2 are the end hydrogen atoms and center 3 is the central hydrogen atom; the internuclear distance between (1, 2) and (2, 3) is 1.765 a.u.

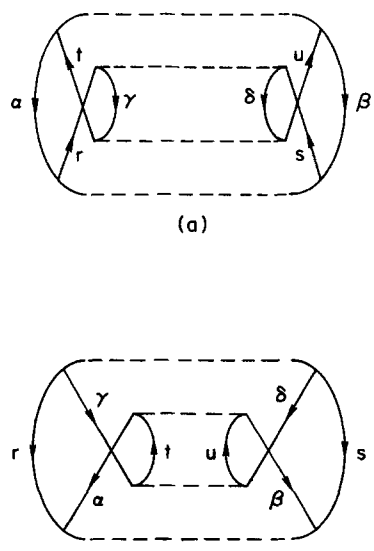

FIG. 19. Quadruple excitation terms arising from overlapping double excitations.

TABLE IV. Correlation energy for linear symmetric H_3.[a,b]

Type of correction	$1\sigma_g 1\sigma_g$	$1\sigma_g 1\sigma_u$	Sum
ΔE^d_{cp}			−0.01903
ΔE_{cp}			−0.02013
$\Delta E^q_{(\alpha\beta)}$ [Eq. (40)]	−0.02597	−0.01534	−0.04131
$\Delta E^r_{(\alpha\beta)}$ [Eq. (49)]	−0.02565	−0.01523	−0.04088
$\Delta E_{(\alpha\beta)}$ [Eq. (33)]	−0.02482	−0.01444	−0.03926
ΔE^d_{CR} [Eq. (62)]			−0.04051
$\Delta E^q_{(\alpha\beta)} + \Delta E^d_{cp}$			−0.05991
$\Delta E_{(\alpha\beta)} + \Delta E_{cp}$			−0.05939
$\Delta E'_{(\alpha\beta)} + \Delta E_{cp}$			−0.05859[c]
CI including singles and doubles			−0.05753
Full CI for basis set			−0.05803

[a]Energies in atomic units.
[b]The near neighbor HH distance is 1.765 a.u.
[c]For the method used to obtain $\Delta E'_{(\alpha\beta)}$, see text.

the single particle excitations are neglected. Both the diagonal approximation, $\Delta E^q_{(\alpha\beta)}$, and the diagonal approximation including rearrangements, $\Delta E^r_{(\alpha\beta)}$, are close to the full pair theory result; the first overestimates it by 5% and the second by 4%. Both the $(1\sigma_g, 1\sigma_g)$ and the $(1\sigma_g, 1\sigma_u)$ pair contributions are seen to be important and they behave correspondingly in the approximate calculations. The total of the core polarization terms and the pair terms overestimate the CI correlation energy by 2% for the full expression $(\Delta E_{cp} + \Delta E_{(\alpha\beta)})$ and by 3% in the diagonal approximation, $(\Delta E^d_{cp} + \Delta E^d_{(\alpha\beta)})$. Thus, an excellent approximation to the CI energy is obtained by use of the diagrammatic technique. The diagonal approximation to the coupled pair energy given by Eq. (62), which excludes the explicit coupling term, C_{12}, of Eq. (71), is seen to yield a value significantly smaller (0.00080 a.u.) than the corresponding diagonal approximation to the sum of the separate pair energies, $\Delta E^d_{(\alpha\beta)}$. Approximately the same correction for pair coupling should apply to $\Delta E_{(\alpha\beta)}$, since the two types of improvements $(\Delta E^d_{(\alpha\beta)} - \Delta E_{(\alpha\beta)}$ and $\Delta E^d_{(\alpha\beta)} - \Delta E^d_{CR})$ are essentially independent. The resulting value for the correlation energy $(\Delta E'_{(\alpha\beta)} + \Delta E_{cp})$, where $\Delta E'_{(\alpha\beta)} \equiv \Delta E_{(\alpha\beta)} + (\Delta E^d_{CR} - \Delta E^d_{(\alpha\beta)})$, is in very good agreement with the complete CI calculation. Finally, we list the correlation energy obtained from CI calculation including only single and double excitations. It can be seen from this that the neglect of triple excitations yields an error of about 1%.

TABLE V. Extended basis set for Li_2 calculation.[a]

Orbital	Exponent
$1s_\sigma$	2.3335
$1s'_\sigma$	4.3950
$2s_\sigma$	0.665
$3s_\sigma$	1.533
$3s'_\sigma$	2.703
$2p_\sigma$	0.740
$2p'_\sigma$	2.2844
$3d_\sigma$	1.1510
$4f_\sigma$	1.252
$2p_\pi$	0.696
$2p_\pi$	1.090
$3d_\pi$	0.500
$3d_\delta$	1.000

$E_{HF} = -14.87183$ a.u.

[a]The internuclear distance is 5.25 a.u.

TABLE VI. Correlation energy of Li_2 with extended basis set.[a,b]

ϵ_2	−0.05440
ϵ_3	−0.00641
$\epsilon_2 + \epsilon_3$	−0.06080
$\Delta E^q_{(\alpha\beta)}$ [Eq. (40)]	−0.07968
$\Delta E^r_{(\alpha\beta)}$ [Eq. (49)]	−0.07409
ΔE^d_{CR} [Eq. (62)]	−0.06976
Experimental correlation energy[c]	−0.1224

[a]Energies in atomic units.
[b]Internuclear distance is 5.25 a.u.
[c]Taken from the empirical curve of H. M. Hulbert and J. O. Hirschfelder, J. Chem. Phys. 9, 61 (1941); 35, 1901 (1961).

B. Extended basis set calculations

Li_2 molecule

The extended basis set for the lithium molecule consisted of nine σ orbitals, three π orbitals, and one δ orbital on each center. The orbital exponents, given in Table V, were chosen as a weighted average of the gerade and ungerade exponents given by Das and Wahl[41]; in addition one d_π and one d_δ orbital were included for extra angular correlation. The Hartree–Fock energy of the basis is also listed in Table V. Although this basis is fairly large, it is not large enough (i.e., not enough high exponent orbitals) to obtain an accurate inner-shell contribution to the correlation energy (see below).

In Table VI we present the second and third pert-order energies, the second-order Epstein–Nesbet result $(\Delta E^q_{(\alpha\beta)})$, the diagonal pair energy $(\Delta E^r_{(\alpha\beta)})$, and the diagonal approximation to the CI matrix including only double excitations (ΔE^d_{CR}). The experimental estimate for the correlation energy is also given in the table. The Rayleigh–Schrödinger series does not converge rapidly, although the convergence appears better than in the small basis set calculation (see Table II). The Epstein-Nesbet and diagonal particle approximation to the pair energy give similar results, between 60% and 65% of the experimental correlation energy. The value obtained from the diagonal approximation to the CI double excitation matrix is somewhat smaller. Since the only difference between $\Delta E^r_{(\alpha\beta)}$ and ΔE^d_{CR} is the inclusion of unlinked diagrams in the latter, it is

TABLE VII. Correlation energy contributions for Li_2 with extended basis set.[a,b]

Term	$\Delta E^d_{(\alpha\beta)}$	$\Delta E^r_{(\alpha\beta)}$
$(1\sigma, 1\sigma)$	−0.03603	−0.03601
$(1\sigma, 2\sigma_g)$	−0.00306	−0.00306
$(2\sigma_g, 2\sigma_g)$	−0.04059	−0.03502

[a]Energies in atomic units.
[b]Internuclear distance is 5.25 a.u.

demonstrated here that these unlinked diagrams can be significant. Furthermore, because the unlinked diagrams are canceled in higher order, $\Delta E^r_{(\alpha\beta)}$ is expected to be more accurate than ΔE^d_{CR}; this conclusion has been confirmed in calculations on polyenes.[42]

It is clear that the extended basis set used here is not sufficient to obtain the full correlation energy of the Li_2 molecule. To determine the origin of the basis set deficiency, we consider the diagonal pair energies given in Table VII; to simplify the table we have summed over the $1\sigma_g$ and $1\sigma_u$ contributions as well as over the different spins. It is seen that the sum of the inner-shell terms $(1\sigma, 1\sigma)$ is about half of the value on the order of −0.073 a.u. expected for two such doubly occupied $1s$-like orbitals. The absence of functions with large exponents in the basis set is probably the source of this difference between the calculated and expected correlation energy. If one takes account of this error in the inner-shell value, it appears that the valence-shell $(2\sigma_g, 2\sigma_g)$ pair energy is well approximated by the present calculation.

TABLE VIII. Extended basis set for N_2.[a]

Orbital	Exponent	Orbital	Exponent
$1s_\sigma$	10.62172	$2p_\pi$	14.626
$1s'_\sigma$	6.00887	$2p'_\pi$	7.61151
$2s_\sigma$	2.54516	$2p''_\pi$	3.26852
$2s'_\sigma$	1.58871	$2p'''_\pi$	1.8951
$2s''_\sigma$	14.626	$2p''''_\pi$	1.22223
$3s_\sigma$	7.31105	$3d_\pi$	19.501
$3s'_\sigma$	19.501	$3d'_\pi$	1.68328
$2p_\sigma$	14.626	$3d''_\pi$	2.91681
$2p'_\sigma$	7.61551	$3d'''_\pi$	5.51063
$2p''_\sigma$	3.26852	$4f_\pi$	24.377
$2p'''_\sigma$	1.8951	$4f'_\pi$	2.81173
$2p''''_\sigma$	1.22223	$3d_\delta$	19.501
$3d_\sigma$	19.501	$3d'_\delta$	1.68328
$3d'_\sigma$	1.68328	$3d''_\delta$	2.91681
$3d''_\sigma$	2.91681	$3d'''_\delta$	5.52063
$3d'''_\sigma$	5.52063	$4f_\delta$	24.377
$4f_\sigma$	24.377	$4f'_\delta$	2.81173
$4f'_\sigma$	2.81173	$4f_\phi$	24.377
		$4f'_\phi$	2.81173

$E_{HF} = -108.99180$ a.u.

[a]Internuclear distance is 2.068 a.u.

TABLE IX. Pair energies for the nitrogen molecule.[a]

Pair$_{(\alpha\beta)}$[b]		$\epsilon_2^{(\alpha\beta)}$	$\Delta E^d_{(\alpha\beta)}$	$\Delta E^r_{(\alpha\beta)}$	Grimaldi[c]
$1\sigma_g^+$	$1\sigma_g^-$	−0.01871	−0.01913	−0.01913	−0.012511
$1\sigma_g$	$2\sigma_g$	−0.00328	−0.00341	−0.00341	−0.002124
$1\sigma_g$	$3\sigma_g$	−0.00329	−0.00344	−0.00344	−0.002035
$1\sigma_g$	$1\sigma_u$	−0.03741	−0.03825	−0.03824	−0.024972
$1\sigma_g$	$2\sigma_u$	−0.00296	−0.00308	−0.00308	−0.002060
$1\sigma_g$	$1\pi_u$	−0.00572	−0.00600	−0.00600	−0.002316
$2\sigma_g^+$	$2\sigma_g^-$	−0.01307	−0.01498	−0.01494	−0.010715
$2\sigma_g$	$3\sigma_g$	−0.01406	−0.01690	−0.01689	−0.011391
$2\sigma_g$	$1\sigma_u$	−0.00332	−0.00346	−0.00346	−0.002123
$2\sigma_g$	$2\sigma_u$	−0.00940	−0.01129	−0.01128	−0.008052
$2\sigma_g$	$1\pi_u$	−0.06344	−0.07693	−0.07671	−0.036315
$3\sigma_g^+$	$3\sigma_g^-$	−0.01596	−0.02034	−0.02017	−0.014130
$3\sigma_g$	$1\sigma_u$	−0.00335	−0.00351	−0.00351	−0.002086
$3\sigma_g$	$2\sigma_u$	−0.02713	−0.03328	−0.03314	−0.024938
$3\sigma_g$	$1\pi_u$	−0.06890	−0.09071	−0.09029	−0.047811
$1\sigma_u^+$	$1\sigma_u^-$	−0.01877	−0.01919	−0.01918	−0.012553
$1\sigma_u$	$2\sigma_u$	−0.00300	−0.00313	−0.00313	−0.002091
$1\sigma_u$	$1\pi_u$	−0.00545	−0.00572	−0.00572	−0.002264
$2\sigma_u^+$	$2\sigma_u^-$	−0.01587	−0.02121	−0.02098	−0.014605
$2\sigma_u$	$1\pi_u$	−0.05131	−0.06745	−0.06719	−0.029974
$1\pi_{u_1}$	$1\pi_{u_{-1}}$	−0.08326	−0.13472	−0.13048	−0.074410
$1\pi_{u_1}$	$1\pi_{u_1}$	−0.05611	−0.08848	−0.08540	−0.034327

[a]The internuclear distance is 2.068 a.u.
[b]Plus and minus superscripts represent spin states. If there is no superscript, the sum of all spin states is assumed.
[c]Reference 46.

N_2 molecule

The basis set used for the nitrogen molecule calculations consisted of eighteen σ, eleven π, six δ, and two ϕ orbitals on each center. The exponents, given in Table VIII, were taken from the atomic exponents of Huzinaga, McWilliams, and Domsky,[43] a weighted average of p_π and d_π gerade and ungerade exponents given by Cade, Sales, and Wahl,[44] and large exponent p, d, and f functions chosen so that the radial maxima matched the orbitals used by Nesbet in his calculation of inner-shell correlation energy of the nitrogen atom.[45] The Hartree–Fock–Roothaan energy given in Table VIII is near that obtained by Cade, Sales, and Wahl,[44] so that the basis set appears to be at the Hartree-Fock limit.

In Table IX we give the pair energies calculated for the nitrogen molecule in various approximations; to save space, we have summed over the different spin orientations for each pair. In addition to the second pert-order, $(\epsilon_2^{(\alpha\beta)})$, Epstein–Nesbet perturbation theory $(\Delta E^d_{(\alpha\beta)})$, and diagonal pair energies $(\Delta E^r_{(\alpha\beta)})$, we give

TABLE X. Correlation energy of the nitrogen molecule.[a]

ϵ_2	−0.52375
$\Delta E^d_{(\alpha\beta)}$	−0.68459
$\Delta E^r_{(\alpha\beta)}$	−0.67577
ΔE^d_{CR}	−0.56029
Experimental correlation energy[b]	−0.554

[a]Internuclear distance is 2.068 a.u.; energy in atomic units.
[b]Reference 46.

the second pert-order energies calculated by Grimaldi.[46] The difference between the second pert-order energies obtained here and by Grimaldi arises from the fact that he used a smaller and less flexible basis set. Unlike the Li_2 calculation, the valence shells do not dominate the correlation energy in this system, which indicates the basis we have used is fairly complete. From Table X, we see that the difference between $\Delta E^d_{(\alpha\beta)}$ and $\Delta E^r_{(\alpha\beta)}$ due to the rearrangement terms is small. Both significantly overestimate the correlation energy; e.g., the diagonal pair energy ($\Delta E^r_{(\alpha\beta)}$) overestimates the experimental correlation energy by 22%. This is a consequence both of the independent pair approximation and the diagonal approximation. We list the results also for a correlation calculation (ΔE^d_{CR}), where we have made the diagonal approximation to the doubly excited CI matrix. In this approximation, we find 101% of the experimental correlation energy.

ACKNOWLEDGMENTS

We thank Dr. H. Keith McDowell and Dr. Attila Szabo for many stimulating and interesting discussions during the course of this work. We thank Dr. R. M. Stevens for use of his diatomic and polyatomic wavefunction programs. We thank Dr. A. D. McLean for the use of his linear molecule wavefunction program. We thank Dr. Sheldon Green and Dr. Patrick Thaddeus for help and hospitality at the Goddard Institute for Space Studies where some of the calculations on N_2 were carried out. We thank Dr. Neil Ostlund for performing the minimum basis CI calculations on Li_2 for us.

APPENDIX: DEMONSTRATION OF THE CANCELLATION OF THE UNLINKED DIAGRAMS FROM THE DOUBLE AND QUADRUPLE EXCITATIONS

In this appendix we show that the quadruple excitation contributions contain terms that cancel the unlinked terms from the double excitation contributions. Although this cancellation has been discussed by Kelly,[26] it is useful to consider it in terms of the partitioned CI matrix. We use the configuration interaction matrix

$$\begin{bmatrix} 0 & \mathbf{B} & 0 \\ \mathbf{B}^+ & \mathbf{D} & \mathbf{C} \\ 0 & \mathbf{C}^+ & \mathbf{Q} \end{bmatrix} \begin{bmatrix} 1 \\ f_2 \\ f_4 \end{bmatrix} = \Delta E_Q \begin{bmatrix} 1 \\ \mathbf{f}_2 \\ \mathbf{f}_4 \end{bmatrix} , \tag{A1}$$

where B contains the coupling matrix elements between the ground state and the double excitations, **D** contains the matrix elements between the double excitations, **C** is the matrix that couples the double excitations to the quadruple excitations, **Q** contains the matrix elements between the quadruple excitations, $\mathbf{f}_2$ is the vector of the double excitation coefficients, and $\mathbf{f}_4$ is the vector of the quadruple excitation coefficients. Solving for $\mathbf{f}_4$, we obtain

$$\mathbf{f}_4 = (\Delta E_Q \mathbf{I} - \mathbf{Q})^{-1} \mathbf{C}^+ \mathbf{f}_2 \tag{A2}$$

From Eqs. (A1) and (A2), we have

$$\mathbf{f}_2 = \left(\Delta E_Q \mathbf{I} - \mathbf{D} - \mathbf{C} \frac{1}{\Delta E_Q \mathbf{I} - \mathbf{Q}} \mathbf{C}^+ \right)^{-1} \mathbf{B}^+ . \tag{A3}$$

and

$$\Delta E_Q = \mathbf{B} \left(\Delta E_Q \mathbf{I} - \mathbf{D} - \mathbf{C} \frac{1}{\Delta E_Q \mathbf{I} - \mathbf{Q}} \mathbf{C}^+ \right)^{-1} \mathbf{B}^+ . \tag{A4}$$

Expanding the denominator of Eq. (A4), we find

$$\Delta E_Q = \mathbf{B} \frac{1}{\Delta E_Q \mathbf{I} - \mathbf{D}} \mathbf{B}^+ + \mathbf{B} \frac{1}{\Delta E_Q \mathbf{I} - \mathbf{D}} \times \mathbf{C} \frac{1}{\Delta E_Q \mathbf{I} - \mathbf{Q}} \mathbf{C}^+ \frac{1}{\Delta E_Q \mathbf{I} - \mathbf{D}} \mathbf{B}^+ + \cdots . \tag{A5}$$

In the approximation that $\Delta E_Q \cong \Delta E_d$, the first term on the right-hand side of Eq. (A5) is the double excitation CI result. As we saw in the main text, this term contains unlinked contributions. To determine the origin of the cancellations of the unlinked terms in Eq. (A5), we expand with respect to the ΔE_Q contributions in the denominators and obtain

$$\Delta E_Q = \left[\mathbf{B} \frac{1}{-\mathbf{D}} \mathbf{B}^+ - \Delta E_Q \mathbf{B} \left(\frac{1}{-\mathbf{D}} \right)^2 \mathbf{B}^+ + (\Delta E_Q)^2 \mathbf{B} \left(\frac{1}{-\mathbf{D}} \right)^3 \mathbf{B}^+ + \cdots \right] + \left[\mathbf{B} \frac{1}{-\mathbf{D}} \mathbf{C} \frac{1}{-\mathbf{Q}} \mathbf{C}^+ \frac{1}{-\mathbf{D}} \mathbf{B}^+ - \Delta E_Q \left\{ \mathbf{B} \left(\frac{1}{-\mathbf{D}} \right)^2 \mathbf{C} \frac{1}{-\mathbf{Q}} \mathbf{C}^+ \frac{1}{-\mathbf{D}} \mathbf{B}^+ + \mathbf{B} \frac{1}{-\mathbf{D}} \mathbf{C} \left(\frac{1}{-\mathbf{Q}} \right)^2 \mathbf{C}^+ \frac{1}{-\mathbf{D}} \mathbf{B}^+ + \mathbf{B} \frac{1}{-\mathbf{D}} \mathbf{C} \frac{1}{-\mathbf{Q}} \mathbf{C}^+ \left(\frac{1}{-\mathbf{D}} \right)^2 \mathbf{B}^+ \right\} + \cdots \right] + \mathbf{B} \frac{1}{-\mathbf{D}} \mathbf{C} \frac{1}{-\mathbf{Q}} \mathbf{C}^+ \frac{1}{-\mathbf{D}} \mathbf{C} \frac{1}{-\mathbf{Q}} \mathbf{C}^+ \frac{1}{-\mathbf{D}} \mathbf{B}^+ + \cdots \tag{A6}$$

To simplify the discussion, we focus on the unlinked terms arising from the excitations involving the two determinants $|\Phi^{rs}_{\alpha\beta}\rangle$ and $|\Phi^{tu}_{\gamma\delta}\rangle$ considered in the main text. It is the second term on the right-hand side of Eq. (A6) that contains the lowest pert-order unlinked contributions. This term gives

$$T_2 = -\mathbf{B} \left(\frac{1}{-\mathbf{D}} \right)^2 \mathbf{B}^+ \Delta E_Q = -\mathbf{B} \left(\frac{1}{-\mathbf{D}} \right)^2 \mathbf{B}^+ \left[\mathbf{B} \frac{1}{-\mathbf{D}} \mathbf{B}^+ - \Delta E_Q \mathbf{B} \left(\frac{1}{-\mathbf{D}} \right)^2 \mathbf{B}^+ + \cdots + \mathbf{B} \frac{1}{-\mathbf{D}} \mathbf{C} \frac{1}{-\mathbf{Q}} \mathbf{C}^+ \frac{1}{-\mathbf{D}} \mathbf{B}^+ + \cdots \right] . \tag{A7}$$

Considering only the first term in the square brackets, we have

$$T_2 \cong \left[-\mathbf{B}^{rs}_{\alpha\beta} \left(\frac{1}{-\mathbf{D}^{rs}_{\alpha\beta}} \right)^2 \mathbf{B}^{+rs}_{\alpha\beta} - \mathbf{B}^{tu}_{\gamma\delta} \left(\frac{1}{-\mathbf{D}^{tu}_{\gamma\delta}} \right)^2 \mathbf{B}^{+tu}_{\gamma\delta} \right] \left[\mathbf{B}^{rs}_{\alpha\beta} \frac{1}{-\mathbf{D}^{rs}_{\alpha\beta}} \mathbf{B}^{+rs}_{\alpha\beta} + \mathbf{B}^{tu}_{\gamma\delta} \frac{1}{-\mathbf{D}^{tu}_{\gamma\delta}} \mathbf{B}^{+tu}_{\gamma\delta} \right] \tag{A8}$$

$$\cong -\frac{\langle rs|v|\tilde{\alpha\beta}\rangle\langle\alpha\beta|v|rs\rangle}{(\epsilon_\alpha+\epsilon_\beta-\epsilon_r-\epsilon_s)^2}\times\frac{\langle rs|v|\tilde{\alpha\beta}\rangle\langle\alpha\beta|v|rs\rangle}{(\epsilon_\alpha+\epsilon_\beta-\epsilon_r-\epsilon_s)}-\frac{\langle tu|v|\tilde{\gamma\delta}\rangle\langle\gamma\delta|v|tu\rangle}{(\epsilon_\gamma+\epsilon_\delta-\epsilon_t-\epsilon_u)^2}\times\frac{\langle tu|v|\tilde{\gamma\delta}\rangle\langle\gamma\delta|v|tu\rangle}{(\epsilon_\gamma+\epsilon_\delta-\epsilon_t-\epsilon_u)}$$
$$-\frac{\langle rs|v|\tilde{\alpha\beta}\rangle\langle\alpha\beta|v|rs\rangle}{(\epsilon_\alpha+\epsilon_\beta-\epsilon_r-\epsilon_s)^2}\times\frac{\langle tu|v|\tilde{\gamma\delta}\rangle\langle\gamma\delta|v|tu\rangle}{(\epsilon_\gamma+\epsilon_\delta-\epsilon_t-\epsilon_u)}-\frac{\langle tu|v|\tilde{\gamma\delta}\rangle\langle\gamma\delta|v|tu\rangle}{(\epsilon_\gamma+\epsilon_\delta-\epsilon_t-\epsilon_u)^2}\times\frac{\langle rs|v|\tilde{\alpha\beta}\rangle\langle\alpha\beta|v|rs\rangle}{(\epsilon_\alpha+\epsilon_\beta-\epsilon_r-\epsilon_s)}\quad . \tag{A9}$$

since

$$B^{rs}_{\alpha\beta}\equiv\langle\Phi^{rs}_{\alpha\beta}|H|\Phi_0\rangle=\langle rs|v|\tilde{\alpha\beta}\rangle\ . \tag{A10}$$

and

$$D^{rs}_{\alpha\beta}\equiv\langle\Phi^{rs}_{\alpha\beta}|H|\Phi^{rs}_{\alpha\beta}\rangle-E_0\cong\epsilon_\alpha+\epsilon_\beta-\epsilon_r-\epsilon_s\ . \tag{A11}$$

In Eq. (A9) we have included only exchanges for two out of the four matrix elements occurring in each term, so that in summing over distinct configurations we will avoid overcounting. This is consistent with the notation used in the main text [see Eq. (17)]. The first two terms in Eq. (A9) are linked pair rearrangement terms and the last two terms are unlinked. The cancellation of the latter terms is due to the fourth term on the right-hand side of Eq. (A6). We again limit the terms to the two double excitations considered previously and include only one quadruply excited function $|\Phi^{rstu}_{\alpha\beta\gamma\delta}\rangle$. The resulting contribution is

$$T_3=\mathbf{B}\frac{1}{-\mathbf{D}}\mathbf{C}\frac{1}{-\mathbf{Q}}\mathbf{C}^+\frac{1}{-\mathbf{D}}\mathbf{B}^+=B^{rs}_{\alpha\beta}\frac{1}{-D^{rs}_{\alpha\beta}}C^{rs,rstu}_{\alpha\beta,\alpha\beta\gamma\delta}\frac{1}{-Q^{rstu}_{\alpha\beta\gamma\delta}}\left[C^{+rs,rstu}_{\alpha\beta,\alpha\beta\gamma\delta}\frac{1}{-D^{rs}_{\alpha\beta}}B^{+rs}_{\alpha\beta}+C^{+tu,rstu}_{\gamma\delta,\alpha\beta\gamma\delta}\frac{1}{-D^{tu}_{\gamma\delta}}B^{+tu}_{\gamma\delta}\right]$$
$$+B^{tu}_{\gamma\delta}\frac{1}{-D^{tu}_{\gamma\delta}}C^{tu,rstu}_{\gamma\delta,\alpha\beta\gamma\delta}\frac{1}{-Q^{rstu}_{\alpha\beta\gamma\delta}}\left[C^{+rs,rstu}_{\alpha\beta,\alpha\beta\gamma\delta}\frac{1}{-D^{rs}_{\alpha\beta}}B^{+rs}_{\alpha\beta}+C^{+tu,rstu}_{\gamma\delta,\alpha\beta\gamma\delta}\frac{1}{-D^{tu}_{\gamma\delta}}B^{+tu}_{\gamma\delta}\right], \tag{A12}$$

where

$$C^{rs,rstu}_{\alpha\beta,\alpha\beta\gamma\delta}=\langle\Phi^{rs}_{\alpha\beta}|H|\Phi^{rstu}_{\alpha\beta\gamma\delta}\rangle=\langle tu|v|\tilde{\gamma\delta}\rangle\ , \tag{A13}$$

and

$$Q^{rstu}_{\alpha\beta\gamma\delta}=\langle\Phi^{rstu}_{\alpha\beta\gamma\delta}|H|\Phi^{rstu}_{\alpha\beta\gamma\delta}\rangle-E_0\cong\epsilon_\alpha+\epsilon_\beta+\epsilon_\gamma+\epsilon_\delta-\epsilon_r-\epsilon_s-\epsilon_t-\epsilon_u\ . \tag{A14}$$

The first term yields

$$\frac{\langle rs|v|\tilde{\alpha\beta}\rangle\langle tu|v|\tilde{\gamma\delta}\rangle}{(\epsilon_\alpha+\epsilon_\beta-\epsilon_r-\epsilon_s)(\epsilon_\alpha+\epsilon_\beta+\epsilon_\gamma+\epsilon_\delta-\epsilon_r-\epsilon_s-\epsilon_t-\epsilon_u)}\left[\frac{\langle\tilde{\gamma\delta}|v|tu\rangle\langle\tilde{\alpha\beta}|v|rs\rangle}{(\epsilon_\alpha+\epsilon_\beta-\epsilon_r-\epsilon_s)}+\frac{\langle\tilde{\alpha\beta}|v|rs\rangle\langle\tilde{\gamma\delta}|v|tu\rangle}{(\epsilon_\gamma+\epsilon_\delta-\epsilon_t-\epsilon_u)}\right] \tag{A15}$$
$$=\frac{\langle rs|v|\tilde{\alpha\beta}\rangle\langle\tilde{\alpha\beta}|v|rs\rangle\langle tu|v|\tilde{\gamma\delta}\rangle\langle\tilde{\gamma\delta}|v|tu\rangle}{(\epsilon_\alpha+\epsilon_\beta-\epsilon_r-\epsilon_s)^2(\epsilon_\gamma+\epsilon_\delta-\epsilon_t-\epsilon_u)} \tag{A16}$$

which cancels the third term in Eq. (A9). The fourth term in Eq. (A9) is similarly cancelled by the second term in Eq. (A12). Thus, all unlinked terms of fourth pert-order (two orders in ΔE_Q) cancel.

We next consider the sixth pert-order terms (three orders in ΔE_Q). The terms from the pure double excitation part are found in the third term on the right hand side of Eq. (A6) and the second term in Eq. (A7). With the same simplifications as employed previously, the term from Eq. (A6) can be written

$$\mathbf{B}\left(\frac{1}{-\mathbf{D}}\right)^3\mathbf{B}^+(\Delta E_Q)^2\cong\mathbf{B}\left(\frac{1}{-\mathbf{D}}\right)^3\mathbf{B}^+\left[\mathbf{B}\frac{1}{-\mathbf{D}}\mathbf{B}^+\right]^2\cong\left[B^{rs}_{\alpha\beta}\left(\frac{1}{-D^{rs}_{\alpha\beta}}\right)^3B^{+rs}_{\alpha\beta}+B^{tu}_{\gamma\delta}\left(\frac{1}{-D^{tu}_{\gamma\delta}}\right)^3B^{+tu}_{\gamma\delta}\right]\left[B^{rs}_{\alpha\beta}\frac{1}{-D^{rs}_{\alpha\beta}}B^{+rs}_{\alpha\beta}+B^{tu}_{\gamma\delta}\frac{1}{-D^{tu}_{\gamma\delta}}B^{+tu}_{\gamma\delta}\right]^2 \tag{A17}$$

The unlinked terms in Eq. (A17) are

$$\frac{2\langle rs|v|\tilde{\alpha\beta}\rangle\langle\alpha\beta|v|rs\rangle\langle rs|v|\tilde{\alpha\beta}\rangle\langle\alpha\beta|v|rs\rangle\langle tu|v|\tilde{\gamma\delta}\rangle\langle\gamma\delta|v|tu\rangle}{(\epsilon_\alpha+\epsilon_\beta-\epsilon_r-\epsilon_s)^4(\epsilon_\gamma+\epsilon_\delta-\epsilon_t-\epsilon_u)}+\frac{\langle rs|v|\tilde{\alpha\beta}\rangle\langle\alpha\beta|v|rs\rangle\langle tu|v|\tilde{\gamma\delta}\rangle\langle\gamma\delta|v|tu\rangle\langle tu|v|\tilde{\gamma\delta}\rangle\langle\gamma\delta|v|tu\rangle}{(\epsilon_\alpha+\epsilon_\beta-\epsilon_r-\epsilon_s)^3(\epsilon_\gamma+\epsilon_\delta-\epsilon_t-\epsilon_u)^2} \tag{A18}$$

plus the two terms obtained from Eq. (A18) by exchanging $\alpha\beta$ with $\gamma\delta$ and rs with tu. The second term in Eq. (A7) gives

$$\left[\mathbf{B}\left(\frac{1}{-\mathbf{D}}\right)^2\mathbf{B}^+\right]^2\Delta E_Q\cong\left[\mathbf{B}\left(\frac{1}{-\mathbf{D}}\right)^2\mathbf{B}^+\right]^2\left[\mathbf{B}\frac{1}{-\mathbf{D}}\mathbf{B}^+\right]=\left[B^{rs}_{\alpha\beta}\left(\frac{1}{-D^{rs}_{\alpha\beta}}\right)^2B^{+rs}_{\alpha\beta}+B^{tu}_{\gamma\delta}\left(\frac{1}{-D^{tu}_{\gamma\delta}}\right)^2B^{+tu}_{\alpha\beta}\right]^2\left[B^{rs}_{\alpha\beta}\frac{1}{-D^{rs}_{\alpha\beta}}B^{+rs}_{\alpha\beta}+B^{tu}_{\gamma\delta}\frac{1}{-D^{tu}_{\gamma\delta}}B^{+tu}_{\gamma\delta}\right]. \tag{A19}$$

The unlinked terms in Eq. (A19) are

$$\frac{\langle rs|v|\tilde{\alpha\beta}\rangle\langle\alpha\beta|v|rs\rangle\langle rs|v|\tilde{\alpha\beta}\rangle\langle\alpha\beta|v|rs\rangle\langle tu|v|\tilde{\gamma\delta}\rangle\langle\gamma\delta|v|tu\rangle}{(\epsilon_\alpha+\epsilon_\beta-\epsilon_r-\epsilon_s)^4(\epsilon_\gamma+\epsilon_\delta-\epsilon_t-\epsilon_u)}+\frac{\langle rs|v|\tilde{\alpha\beta}\rangle\langle\alpha\beta|v|rs\rangle\langle tu|v|\tilde{\gamma\delta}\rangle\langle\gamma\delta|v|tu\rangle\langle rs|v|\tilde{\alpha\beta}\rangle\langle\alpha\beta|v|rs\rangle}{(\epsilon_\alpha+\epsilon_\beta-\epsilon_r-\epsilon_s)^3(\epsilon_\gamma+\epsilon_\delta-\epsilon_t-\epsilon_u)^2}$$
$$+\frac{\langle rs|v|\tilde{\alpha\beta}\rangle\langle\alpha\beta|v|rs\rangle\langle tu|v|\tilde{\gamma\delta}\rangle\langle\gamma\delta|v|tu\rangle\langle tu|v|\tilde{\gamma\delta}\rangle\langle\gamma\delta|v|tu\rangle}{(\epsilon_\alpha+\epsilon_\beta-\epsilon_r-\epsilon_s)^2(\epsilon_\gamma+\epsilon_\delta-\epsilon_t-\epsilon_u)^3} \tag{A20}$$

plus the three terms obtained from Eq. (A20) by interchanging rs with tu and $\alpha\beta$ with $\gamma\delta$. The terms that cancel

Eq. (A18) and Eq. (A20) occur in the fifth through eighth terms of Eq. (A6) and the third term of Eq. (A7). The contribution from Eq. (A7) is

$$\left[-\mathbf{B}\left(\frac{1}{-\mathbf{D}}\right)^2\mathbf{B}^+\mathbf{B}\frac{1}{-\mathbf{D}}\mathbf{C}\frac{1}{-\mathbf{Q}}\mathbf{C}^+\frac{1}{-\mathbf{D}}\mathbf{B}^+\right] = -\left[B^{rs}_{\alpha\beta}\frac{1}{(-D^{rs}_{\alpha\beta})^2}B^{+rs}_{\alpha\beta}\right]\left\{B^{rs}_{\alpha\beta}\frac{1}{-D^{rs}_{\alpha\beta}}C^{rs,rstu}_{\alpha\beta,\alpha\beta\gamma\delta}\frac{1}{-Q^{rstu}_{\alpha\beta\gamma\delta}}\left[C^{+rs,rstu}_{\alpha\beta,\alpha\beta\gamma\delta}\frac{1}{-D^{rs}_{\alpha\beta}}B^{+rs}_{\alpha\beta}+C^{+tu,rstu}_{\gamma\delta,\alpha\beta\gamma\delta}\frac{1}{-D^{tu}_{\gamma\delta}}B^{+tu}_{\gamma\delta}\right]+B^{tu}_{\gamma\delta}\frac{1}{-D^{tu}_{\gamma\delta}}C^{tu,rstu}_{\gamma\delta,\alpha\beta\gamma\delta}\frac{1}{-Q^{rstu}_{\alpha\beta\gamma\delta}}\left[C^{+rs,rstu}_{\alpha\beta,\alpha\beta\gamma\delta}\frac{1}{-D^{rs}_{\alpha\beta}}B^{+rs}_{\alpha\beta}+C^{+tu,rstu}_{\gamma\delta,\alpha\beta\gamma\delta}\frac{1}{-D^{tu}_{\gamma\delta}}B^{+tu}_{\gamma\delta}\right]\right\} \tag{A21}$$

plus the four terms obtained from Eq. (A21) by exchanging $\alpha\beta$ with $\gamma\delta$ are rs with tu. Writing out the terms of Eq. (A21), we obtain

$$-\frac{\langle rs|v|\tilde{\alpha\beta}\rangle\langle\alpha\beta|v|rs\rangle\langle rs|v|\tilde{\alpha\beta}\rangle\langle\alpha\beta|v|rs\rangle\langle tu|v|\tilde{\gamma\delta}\rangle\langle\gamma\delta|v|tu\rangle}{(\epsilon_\alpha+\epsilon_\beta-\epsilon_r-\epsilon_s)^4(\epsilon_\gamma+\epsilon_\delta-\epsilon_t-\epsilon_u)}-\frac{\langle rs|v|\tilde{\alpha\beta}\rangle\langle\alpha\beta|v|rs\rangle\langle rs|v|\tilde{\alpha\beta}\rangle\langle\alpha\beta|v|rs\rangle\langle tu|v|\tilde{\gamma\delta}\rangle\langle\gamma\delta|v|tu\rangle}{(\epsilon_\alpha+\epsilon_\beta-\epsilon_r-\epsilon_s)^3(\epsilon_\gamma+\epsilon_\delta-\epsilon_t-\epsilon_u)^2} \tag{A22}$$

The fifth, sixth, and seventh terms of Eq. (A6) are

$$\begin{aligned}-\Delta E_Q&\left[\mathbf{B}\left(\frac{1}{-\mathbf{D}}\right)^2\mathbf{C}\frac{1}{-\mathbf{Q}}\mathbf{C}^+\frac{1}{-\mathbf{D}}\mathbf{B}^+ + \mathbf{B}\frac{1}{-\mathbf{D}}\mathbf{C}\left(\frac{1}{-\mathbf{Q}}\right)^2\mathbf{C}^+\frac{1}{-\mathbf{D}}\mathbf{B}^+ + \mathbf{B}\frac{1}{-\mathbf{D}}\mathbf{C}\frac{1}{-\mathbf{Q}}\mathbf{C}^+\left(\frac{1}{-\mathbf{D}}\right)^2\mathbf{B}^+\right]\\ &\cong -\left[B^{rs}_{\alpha\beta}\frac{1}{-D^{rs}_{\alpha\beta}}B^{+rs}_{\alpha\beta}+B^{tu}_{\gamma\delta}\frac{1}{-D^{tu}_{\gamma\delta}}B^{+tu}_{\gamma\delta}\right]\left[B^{rs}_{\alpha\beta}\left(\frac{1}{-D^{rs}_{\alpha\beta}}\right)^2C^{rs,rstu}_{\alpha\beta,\alpha\beta\gamma\delta}\frac{1}{-Q^{rstu}_{\alpha\beta\gamma\delta}}\left(C^{+rs,rstu}_{\alpha\beta,\alpha\beta\gamma\delta}\frac{1}{-D^{rs}_{\alpha\beta}}B^{+rs}_{\alpha\beta}+C^{+tu,rstu}_{\gamma\delta,\alpha\beta\gamma\delta}\frac{1}{-D^{tu}_{\gamma\delta}}B^{+tu}_{\gamma\delta}\right)\right.\\ &+B^{rs}_{\alpha\beta}\frac{1}{-D^{rs}_{\alpha\beta}}C^{rs,rstu}_{\alpha\beta,\alpha\beta\gamma\delta}\left(\frac{1}{-Q^{rstu}_{\alpha\beta\gamma\delta}}\right)^2\left(C^{+rs,rstu}_{\alpha\beta,\alpha\beta\gamma\delta}\frac{1}{-D^{rs}_{\alpha\beta}}B^{+rs}_{\alpha\beta}+C^{+tu,rstu}_{\gamma\delta,\alpha\beta\gamma\delta}\frac{1}{-D^{tu}_{\gamma\delta}}B^{+tu}_{\gamma\delta}\right)\\ &\left.+B^{rs}_{\alpha\beta}\frac{1}{-D^{rs}_{\alpha\beta}}C^{rs,rstu}_{\alpha\beta,\alpha\beta\gamma\delta}\frac{1}{-Q^{rstu}_{\alpha\beta\gamma\delta}}\left(C^{+rs,rstu}_{\alpha\beta,\alpha\beta\gamma\delta}\left(\frac{1}{-D^{rs}_{\alpha\beta}}\right)^2B^{+rs}_{\alpha\beta}+C^{+tu,rstu}_{\gamma\delta,\alpha\beta\gamma\delta}\left(\frac{1}{-D^{tu}_{\gamma\delta}}\right)^2B^{+tu}_{\gamma\delta}\right)\right]\end{aligned} \tag{A23}$$

plus the six terms obtained from Eq. (A23) by exchanging $\alpha\beta$ with $\gamma\delta$ and rs with tu. Combining the terms in Eq. (A23), we obtain

$$\begin{aligned}-\Bigg[&\frac{2\langle rs|v|\tilde{\alpha\beta}\rangle\langle\alpha\beta|v|rs\rangle\langle rs|v|\tilde{\alpha\beta}\rangle\langle\alpha\beta|v|rs\rangle\langle tu|v|\tilde{\gamma\delta}\rangle\langle\gamma\delta|v|tu\rangle}{(\epsilon_\alpha+\epsilon_\beta-\epsilon_r-\epsilon_s)^4(\epsilon_\gamma+\epsilon_\delta-\epsilon_t-\epsilon_u)}\\ &+\frac{\langle rs|v|\tilde{\alpha\beta}\rangle\langle\alpha\beta|v|rs\rangle\langle tu|v|\tilde{\gamma\delta}\rangle\langle\gamma\delta|v|tu\rangle\langle tu|v|\tilde{\gamma\delta}\rangle\langle\gamma\delta|v|tu\rangle}{(\epsilon_\alpha+\epsilon_\beta-\epsilon_r-\epsilon_s)^2(\epsilon_\gamma+\epsilon_\delta-\epsilon_t-\epsilon_u)^3}+\frac{\langle rs|v|\tilde{\alpha\beta}\rangle\langle\alpha\beta|v|rs\rangle\langle tu|v|\tilde{\gamma\delta}\rangle\langle\gamma\delta|v|tu\rangle\langle tu|v|\tilde{\gamma\delta}\rangle\langle\gamma\delta|v|tu\rangle}{(\epsilon_\alpha+\epsilon_\beta-\epsilon_r-\epsilon_s)^3(\epsilon_\gamma+\epsilon_\delta-\epsilon_t-\epsilon_u)^2}\\ &+\frac{\langle rs|v|\tilde{\alpha\beta}\rangle\langle\alpha\beta|v|rs\rangle\langle tu|v|\tilde{\gamma\delta}\rangle\langle\gamma\delta|v|tu\rangle\langle tu|v|\tilde{\gamma\delta}\rangle\langle\gamma\delta|v|tu\rangle}{(\epsilon_\alpha+\epsilon_\beta-\epsilon_r-\epsilon_s)^3(\epsilon_\alpha+\epsilon_\beta+\epsilon_\gamma+\epsilon_\delta-\epsilon_r-\epsilon_s-\epsilon_t-\epsilon_u)(\epsilon_\gamma+\epsilon_\delta-\epsilon_t-\epsilon_u)}\\ &+\frac{\langle rs|v|\tilde{\alpha\beta}\rangle\langle\alpha\beta|v|rs\rangle\langle rs|v|\tilde{\alpha\beta}\rangle\langle\alpha\beta|v|rs\rangle\langle tu|v|\tilde{\gamma\delta}\rangle\langle\gamma\delta|v|tu\rangle}{(\epsilon_\alpha+\epsilon_\beta-\epsilon_r-\epsilon_s)^2(\epsilon_\alpha+\epsilon_\beta+\epsilon_\gamma+\epsilon_\delta-\epsilon_r-\epsilon_s-\epsilon_t-\epsilon_u)(\epsilon_\gamma+\epsilon_\delta-\epsilon_t-\epsilon_u)^2}\Bigg]\ .\end{aligned} \tag{A24}$$

The eighth term in Eq. (A6) is

$$\mathbf{B}\frac{1}{-\mathbf{D}}\mathbf{C}\frac{1}{-\mathbf{Q}}\mathbf{C}^+\frac{1}{-\mathbf{D}}\mathbf{C}\frac{1}{-\mathbf{Q}}\mathbf{C}^+\frac{1}{-\mathbf{D}}\mathbf{B}^+ = B^{rs}_{\alpha\beta}\frac{1}{-D^{rs}_{\alpha\beta}}C^{+rs,rstu}_{\alpha\beta,\alpha\beta\gamma\delta}\frac{1}{-Q^{rstu}_{\alpha\beta\gamma\delta}}\left[C^{+rs,rstu}_{\alpha\beta,\alpha\beta\gamma\delta}\frac{1}{-D^{rs}_{\alpha\beta}}C^{+rs,rstu}_{\alpha\beta,\alpha\beta\gamma\delta}\frac{1}{-Q^{rstu}_{\alpha\beta\gamma\delta}}\left(C^{+rs,rstu}_{\alpha\beta,\alpha\beta\gamma\delta}\frac{1}{-D^{rs}_{\alpha\beta}}B^{+rs}_{\alpha\beta}+C^{+tu,rstu}_{\gamma\delta,\alpha\beta\gamma\delta}\frac{1}{-D^{tu}_{\gamma\delta}}B^{+tu}_{\gamma\delta}\right)+C^{+tu,rstu}_{\gamma\delta,\alpha\beta\gamma\delta}\frac{1}{-D^{tu}_{\gamma\delta}}C^{tu,rstu}_{\gamma\delta,\alpha\beta\gamma\delta}\frac{1}{-Q^{rstu}_{\alpha\beta\gamma\delta}}\left(C^{+rs,rstu}_{\alpha\beta,\alpha\beta\gamma\delta}\frac{1}{-D^{rs}_{\alpha\beta}}B^{+rs}_{\alpha\beta}+C^{+tu,rstu}_{\gamma\delta,\alpha\beta\gamma\delta}\frac{1}{-D^{tu}_{\gamma\delta}}B^{+tu}_{\gamma\delta}\right)\right] \tag{A25}$$

plus the four terms obtained from Eq. (A25) by exchanging $\alpha\beta$ with $\gamma\delta$ and rs with tu. Combining the terms in Eq. (A25), we obtain

$$\begin{aligned}&\frac{\langle\alpha\beta|v|\tilde{rs}\rangle\langle\gamma\delta|v|\tilde{tu}\rangle\langle tu|v|\gamma\delta\rangle\langle\gamma\delta|v|\tilde{tu}\rangle\langle tu|v|\gamma\delta\rangle\langle rs|v|\alpha\beta\rangle}{(\epsilon_\alpha+\epsilon_\beta-\epsilon_r-\epsilon_s)^3(\epsilon_\gamma+\epsilon_\delta-\epsilon_t-\epsilon_u)(\epsilon_\alpha+\epsilon_\beta+\epsilon_\gamma+\epsilon_\delta-\epsilon_r-\epsilon_s-\epsilon_t-\epsilon_u)}\\ &+\frac{\langle\alpha\beta|v|\tilde{rs}\rangle\langle\gamma\delta|v|\tilde{tu}\rangle\langle rs|v|\alpha\beta\rangle\langle\alpha\beta|v|\tilde{rs}\rangle\langle tu|v|\gamma\delta\rangle\langle rs|v|\alpha\beta\rangle}{(\epsilon_\alpha+\epsilon_\beta-\epsilon_r-\epsilon_s)^2(\epsilon_\alpha+\epsilon_\beta+\epsilon_\gamma+\epsilon_\delta-\epsilon_r-\epsilon_s-\epsilon_t-\epsilon_u)(\epsilon_\gamma+\epsilon_\delta-\epsilon_t-\epsilon_u)^2}\ .\end{aligned} \tag{A26}$$

It is clear that the sum of the terms in Eq. (A26), (A24), and (A22) cancel the sum of the terms in Eq. (A18) and (A20).

The above development has shown explicitly that all unlinked terms through order $(\Delta E_Q)^3$ cancel. Corresponding arguments can be used to demonstrate that all orders of ΔE_Q cancel in a corresponding way. For the case of two "nonoverlapping" pair excitations, all the true correlation contributions thus come from double excitations, and the sole effect of quadruple excitations is to cancel the unlinked terms.

In demonstrating the cancellations of unlinked terms in Eq. (A5), we considered only the coupling between the determinants $|\Phi^{rs}_{\alpha\beta}\rangle$ and $|\Phi^{tu}_{\gamma\delta}\rangle$. It is instructive to examine the second term on the right-hand side of Eq. (A5) and include cross terms that arise from a simultaneous consideration of the determinants $|\Phi^{rs}_{\alpha\beta}\rangle$, $|\Phi^{tu}_{\alpha\beta}\rangle$, $|\Phi^{rs}_{\gamma\delta}\rangle$, and $|\Phi^{tu}_{\gamma\delta}\rangle$. For this case in lowest pert-order, we have

$$\mathbf{B}\frac{1}{-\mathbf{D}}\mathbf{C}\frac{1}{-\mathbf{Q}}\mathbf{C}^{+}\frac{1}{-\mathbf{D}}\mathbf{B}^{+} = B^{rs}_{\alpha\beta}\frac{1}{-D^{rs}_{\alpha\beta}}C^{rs,rstu}_{\alpha\beta,\alpha\beta\gamma\delta}\frac{1}{-Q^{rstu}_{\alpha\beta\gamma\delta}} \times\left[C^{+rs,rstu}_{\alpha\beta,\alpha\beta\gamma\delta}\frac{1}{-D^{rs}_{\alpha\beta}}B^{+rs}_{\alpha\beta}+C^{+tu,rstu}_{\gamma\delta,\alpha\beta\gamma\delta}\frac{1}{-D^{tu}_{\gamma\delta}}B^{+tu}_{\gamma\delta}+C^{+tu,rstu}_{\alpha\beta,\alpha\beta\gamma\delta}\frac{1}{-D^{tu}_{\alpha\beta}}B^{+tu}_{\alpha\beta}+C^{+rs,rstu}_{\gamma\delta,\alpha\beta\gamma\delta}\frac{1}{-D^{rs}_{\gamma\delta}}B^{+rs}_{\gamma\delta}\right] \tag{A27}$$

plus the four terms obtained from Eq. (A27) by exchanging $\alpha\beta$ with $\gamma\delta$ and rs with tu. The first two terms of Eq. (A27) are the same as those that appear in Eq. (A12) and are written out in Eq. (A16). The second two terms give

$$\frac{\langle rs\,|\,v\,|\,\tilde{\alpha}\beta\rangle\langle tu\,|\,v\,|\,\tilde{\gamma}\delta\rangle\langle\gamma\delta\,|\,v\,|\,rs\rangle\langle\alpha\beta\,|\,v\,|\,tu\rangle}{(\epsilon_\alpha+\epsilon_\beta-\epsilon_r-\epsilon_s)(\epsilon_\alpha+\epsilon_\beta+\epsilon_\gamma+\epsilon_\delta-\epsilon_r-\epsilon_s-\epsilon_t-\epsilon_u)(\epsilon_\alpha+\epsilon_\beta-\epsilon_t-\epsilon_u)} + \frac{\langle rs\,|\,v\,|\,\tilde{\alpha}\beta\rangle\langle tu\,|\,v\,|\,\tilde{\gamma}\delta\rangle\langle\alpha\beta\,|\,v\,|\,tu\rangle\langle\gamma\delta\,|\,v\,|\,rs\rangle}{(\epsilon_\alpha+\epsilon_\beta-\epsilon_r-\epsilon_s)(\epsilon_\alpha+\epsilon_\beta+\epsilon_\gamma+\epsilon_\delta-\epsilon_r-\epsilon_s-\epsilon_t-\epsilon_u)(\epsilon_\gamma+\epsilon_\delta-\epsilon_r-\epsilon_s)} \tag{A28}$$

These two terms are linked and their direct diagrammatic representation is shown in Fig. 19. These diagrams have exactly the same structure as the linked coupling rearrangement diagrams that arise in the coupling of two pairs with the same two particle states (i.e., if $r=t$ and $s=u$) or the same hole states ($\alpha=\gamma$, $\delta=\beta$).

*Supported in part by a grant from the National Science Foundation.

†IBM Predoctoral Fellow. Present address: Department of Physics, The University of Utah, Salt Lake City, Utah 84112.

[1]C. C. J. Roothaan, Rev. Mod. Phys. 23, 69 (1951).
[2]H. F. Schaefer III, *The Electronic Structure of Atoms and Molecules* (Addison-Wesley, Reading, MA, 1972).
[3]R. K. Nesbet, Adv. Chem. Phys. 14, 1 (1969).
[4]O. Sinanoğlu, Adv. Chem. Phys. 14, 237 (1969).
[5]H. P. Kelly, Adv. Theoret. Phys. 2, 75 (1968).
[6]J. Čižek, J. Chem. Phys. 45, 4256 (1966).
[7]J. D. Doll, Ph. D. thesis, Harvard University, Cambridge, MA, 1971.
[8]J. D. Doll and W. Reinhardt, J. Chem. Phys. 57, 1169 (1972).
[9]H. P. Kelly, Phys. Rev. Lett. 23, 455 (1969).
[10]H. P. Kelly, Phys. Rev. A 1, 274 (1970).
[11]T. Lee, N. C. Dutta, and T. P. Das, Phys. Rev. Lett. 25, 204 (1970).
[12]J. E. Rodgers, T. Lee, T. P. Das, and D. Ikenberry, Phys. Rev. A 7, 51 (1973).
[13]J. H. Miller and H. P. Kelly, Phys. Rev. Lett. 26, 679 (1971).
[14]T. Lee and T. P. Das, Phys. Rev. A 6, 968 (1972).
[15]N. C. Dutta and M. Karplus, Chem. Phys. Lett. 31, 455 (1975).
[16]C. M. Dutta, N. C. Dutta and T. P. Das, Phys. Rev. Lett. 25, 1695 (1970).
[17]J. M. Schulman and D. N. Kaufman, J. Chem. Phys. 53, 477 (1970).
[18]J. M. Schulman and D. N. Kaufman, J. Chem. Phys. 57, 2328 (1972).
[19]R. J. Bartlett and D. M. Silver, Phys. Rev. A 10, 1927 (1974).
[20]R. J. Bartlett and D. M. Silver, J. Chem. Phys. 62, 3258 (1975).
[21]U. Kaldor, J. Chem. Phys. 62, 4634 (1975).
[22]K. F. Freed, Phys. Rev. 173, 1 (1968).
[23]K. F. Freed, Chem. Phys. Lett. 4, 496 (1970).
[24]K. F. Freed, Ann. Rev. Phys. Chem. 22, 313 (1971).
[25]H. P. Kelly and A. M. Sessler, Phys. Rev. 132, 2091 (1963).
[26]H. Kelly, Phys. Rev. 134, A1450 (1964).
[27]P. O. Löwdin, J. Math. Phys. 3, 969 (1962).
[28]J. Goldstone, Proc. R. Soc. (London), A 239, 267 (1957).
[29]N. H. March, W. H. Young, and S. Sampanthar, *The Many-Body Problem in Quantum Mechanics* (Cambridge University, New York, 1967).
[30]O. Sinanoğlu, J. Chem. Phys. 36, 706 (1962).
[31]O. Sinanoğlu, J. Chem. Phys. 36, 3198 (1962).
[32]J. Paldus, J. Čižek, and I. Shavitt, Phys. Rev. A 5, 50 (1972).
[33]M. Karplus and W. P. Reinhardt, *An Introduction to Many-Body Theory with Applications to Atoms and Molecules*, Chap. 7 (to be published).
[34]P. Claverie, S. Diner, and J. P. Malrieu, Int. J. Quantum Chem. 1, 751 (1967).
[35]K. A. Brueckner and D. T. Goldman, Phys. Rev. 117, 207 (1960).
[36]J. H. Miller and H. P. Kelly, Phys. Rev. A 3, 578 (1971).
[37]D. L. Freeman, Ph. D. thesis, Harvard University, Cambridge, MA, 1972.
[38]S. Fraga and B. J. Ransil, J. Chem. Phys. 36, 1127 (1962).
[39]I. Shavitt, R. M. Stevens, F. L. Minn, and M. Karplus, J. Chem. Phys. 48, 2700 (1968).
[40]H. K. McDowell, Ph. D. thesis, Harvard University, Cambridge, MA, 1972.
[41]G. Das and A. C. Wahl, J. Chem. Phys. 44, 87 (1966).
[42]I. Ohmine, N. Dutta, and M. Karplus (to be published).
[43]S. Huzinaga, D. McWilliams, and B. Domsky, J. Chem. Phys. 54, 2283 (1971).
[44]P. E. Cade, K. D. Sales, and A. C. Wahl, J. Chem. Phys. 44, 1973 (1966).
[45]R. K. Nesbet, Phys. Rev. 175, 2 (1968).
[46]F. Grimaldi, J. Chem. Phys. 43, S 59 (1965).